Transient climate effects of large impacts on Titan

Kevin J. Zahnle[a], Donald G. Korycansky[b], Conor A. Nixon[c]

[a] *Space Science Division, NASA Ames Research Center, MS 245-3, Moffett Field CA 94035 USA*
[b] *CODEP, Dept. of Earth Sciences, University of California, Santa Cruz CA 95064, USA*
[c] *Planetary Systems Laboratory, Goddard Space Flight Center, Greenbelt MD 20771, USA*

Abstract

Titan's thick atmosphere and volatile-rich surface cause it to respond to big impacts in a somewhat Earth-like manner. Here we construct a simple globally-averaged model that tracks the flow of energy through the environment in the weeks, years, and millenia after a big comet strikes Titan. The model Titan is endowed with 1.4 bars of N_2 and 0.07 bars of CH_4, methane lakes, a water ice crust, and enough methane underground to saturate the regolith to the surface. We find that a nominal Menrva impact is big enough to raise the surface temperature by ∼80 K and to double the amount of methane in the atmosphere. The extra methane drizzles out of the atmosphere over hundreds of years. An upper-limit Menrva is just big enough to raise the surface to water's melting point. The putative Hotei impact (a possible 800-1200 km diameter basin, Soderblom et al., 2009) is big enough to raise the surface temperature to 350-400 K. Water rain must fall and global meltwaters might range between 50 m to more than a kilometer deep, depending on the details. Global meltwater oceans do not last more than a few decades or centuries at most, but are interesting to consider given Titan's organic wealth. Significant near-surface clathrate formation is possible as Titan cools but faces major kinetic barriers.

Keywords:
Titan, impact basins, atmospheric evolution, methane, liquid water

1. Introduction

It has long been appreciated that a comet big enough to punch through Titan's atmosphere would generate impact melts of liquid water that could persist for considerable periods of time (Thompson and Sagan, 1992; Artemieva and Lunine, 2003,

Email addresses: Kevin.J.Zahnle@NASA.gov (Kevin J. Zahnle), dkorycan@ucsc.edu (Donald G. Korycansky), conor.a.nixon@nasa.gov (Conor A. Nixon)

2005; O'Brien et al., 2005). Water melts on Titan are interesting for many reasons, foremost the likelihood that interesting chemistry takes place when the nitrogenous organic matter expected to be widespread and abundant on Titan's surface is dissolved in liquid water. The chemical picture is somewhat reminiscent of Darwin's warm little ponds, or more closely, Miller and Bada's melt pools on ice. The latter are freezing pools of water that concentrate simple products of atmospheric chemistry like HCN and H_2CO, which combine in interesting ways. This path to the origin of life was featured in Jacob Bronowski's classic television series an companion book, *The Ascent of Man* (Bronowski, 1973).

Previous work has focused on impact-generated crater lakes, sometimes called impact oases. Thompson and Sagan (1992) used generic formulae to estimate volumes of impact melt, whilst Artemieva and Lunine (2003, 2005) computed melt volumes using 3D numerical simulations of impacts into ice. Both groups estimated crater lake lifetimes analytically from the energy balance between the latent heat of fusion (released when water freezes to the bottom of the ice lid) and thermal conduction through the ice lid. Cooling of this kind is slow and crater lakes deeper than 100 m are predicted to long endure. Thompson and Sagan (1992) and Artemieva and Lunine (2003) estimated lake lifetimes as long as $10^4 - 10^6$ years analytically. Artemieva and Lunine (2005) generalized their results to compute the size-frequency-longevity distribution of crater lakes produced by a plausible size-frequency distributions of impacts. They concluded that "a global melt layer at any time after the very beginning of Titan's history is improbable; but transient melting local to newly formed craters has occurred over large parts of the surface."

O'Brien et al. (2005) revisited lake lifetimes using a 2-D numerical heat conduction code. The numerical model considered lakes set on the floor of icy craters. They found that a 15 km diameter crater could sustain a liquid environment for $\sim$ 100 - 1000 years, and a 150 km crater for $\sim 10^3$ – 10^4 years, with the lower bounds corresponding to liquid water and the upper bounds corresponding to an ammonia-water eutectic. These lake lifetimes are about 100-fold shorter than the corresponding analytical estimates. O'Brien et al consider the difference mostly a consequence of their using a more realistic geometry.

Kraus et al. (2011) and Senft and Stewart (2011) used the CTH hydrocode and their "5-phase" equation of state (EOS) for the water substance to perform numerical simulations of impact cratering on Ganymede and Europa. The 5-phase equation of state includes vapor, liquid, ordinary ice, and two high pressure solid phases akin to ices VI and VII. Kraus et al. (2011) predict volumes of impact-generated melt and impact-generated vapor that are consistent with the computations by Artemieva and Lunine and most other previous work.

Senft and Stewart (2011) emphasize the previously neglected role played by high pressure forms of ice. They found that impacts in ice leave "hot plugs" in the middle of the crater where the shock is strong enough to compress ice into a high density polymorph. Senft and Stewart find that compression into the high density phase leaves a great deal more heat in the ice after decompression than previous EOSs. The resulting plug of liquid water and warm ice ($T \approx T_m$) distinguishes the new simulations from previous work done with simpler equations of state. The warm ice plays a key role in the evolution and duration of crater lakes.

Here we will focus on much bigger impacts, impacts big enough to raise the whole surface of Titan to the melting point. In overview, the work we describe here parallels work we have done for impacts on Earth (Sleep et al., 1989; Zahnle, 1990; Melosh et al., 1990; Zahnle and Sleep, 1997; Zahnle et al., 2007; Nisbet et al., 2007) and Mars (Sleep and Zahnle, 1998; Segura et al., 2002). On Earth, big impacts vaporize water that later rains out. This can also happen on Mars, but because the martian atmosphere is thin, the atmosphere stores little of the impact energy; thus Mars is prone to cool quickly. By contrast, Titan's thick atmosphere provides a huge thermal buffer. It takes a big impact to heat it, but once heated it takes a long time to cool down.

2. Big Basins

The biggest known obvious impact feature on Titan is Menrva, a well-preserved ∼444 km diameter impact basin partially seen by Cassini imaging radar (Wood et al., 2010). The next largest known crater is ∼180 km diameter. Menrva is comparable in size to Gilgamesh on Ganymede or Lofn on Callisto, both of which are young in the cosmic sense of post-dating the late bombardment. At current impact rates, Gilgamesh and Lofn would have ages on the order of a billion years based on superposed craters and the contemporary rate of comet impacts (Zahnle et al., 2003; Dones et al., 2009), but the uncertainty effectively embraces the entire history of the Solar System. Menrva's age is also indeterminate. At current impact rates one expects on the order of one Menrva in 4 Gyr on Titan (Dones et al., 2009).

There is evidence of at least one older and bigger crater on Titan. Hotei Regio is a ∼700 km diameter quasi-circular IR albedo feature that appears to lie within a larger basin that in turn appears, at least on the side mapped by radar, to be an arc of a circle (Hotei Arcus). The albedo feature has been a leading candidate for a cryovolcanic flow (Soderblom et al., 2009). Soderblom et al. (2009) suggest that the basin itself is an ancient impact feature, perhaps as large as 1200 km diameter, that has been severely degraded. We will make much of Hotei-scale impacts here.

2.1. Impact energies from crater scaling

Textbook crater scaling is highly suspect for a basin as big as Menrva, let alone Hotei, which makes estimates of impact energies even less certain than usual. Given this caveat, we use formulae for impact craters in the gravity-scaling limit derived from experimental Π-group relations by Schmidt and Housen (1987) as expressed by Zahnle et al. (2008). The cratering efficiency Π_V goes as

$$\Pi_V \equiv \frac{\rho_t V_{ap}}{m_i} = 0.2\,\Pi_2^{-0.65}\cos\theta, \tag{1}$$

where

$$\Pi_2 \equiv \frac{2g}{v_i^2}\left(\frac{m_i}{\rho_i}\right)^{1/3}. \tag{2}$$

The apparent volume V_{ap} in Eq (1) is measured with respect to the original surface. In these expressions ρ_i and ρ_t denote the densities of the projectile and target, m_i, v_i, and d_i denote the mass, impact velocity, and diameter of the projectile, and g is the surface gravity. The dependence on incidence angle θ (measured from the vertical) is that recommended by Melosh (1989). We assume the apparent crater can be described as a paraboloid with a depth/diameter ratio of 0.15, which gives

$$D_{ap} = 1.1\left(\frac{\rho_i}{\rho_t}\right)^{1/3}\left(\frac{v_i^2}{g}\right)^{0.22} d_i^{0.78}\cos^{1/3}\theta. \tag{3}$$

as the diameter D_{ap} of the apparent crater. The rim-to-rim diameter D of simple craters is about 7% wider than the apparent crater (which is measured with respect to the original surface). The depth/diameter ratio of complex craters is often written $(D/D_c)^{-0.4}$, where $D > D_c$ is the transitional diameter for the transition from simple to complex craters. The result is

$$D = 1.07 D_{ap}\,(D_{ap}/D_c)^{0.15} \qquad D > D_c. \tag{4}$$

We use $D_c = 2.5$ km for Titan. These formulae are very similar to those used by Artemieva and Lunine (2005).

It is interesting to compare these scalings to a new set of crater-scaling parameters for icy satellites derived by Kraus et al. (2011) directly from their hydrocode simulations. The new formulae should be more appropriate to real craters in ice, because the older Schmidt-Housen parameterization is scaled from small craters in rock and sand. However, at least for big impacts on Titan, the Kraus et al. (2011) prescription gives very nearly the same relationship between the impactor's diameter

and the resulting final crater diameter as that given here. Indeed, for the putative 1200 km Hotei basin, the Kraus et al. (2011) prescription gives the same impactor diameter as Eq (4) to 3 digits. The coincidence is of course purely accidental, but amusing and perhaps reassuring.

For the specific case of nominal Menrva we use $\theta = 30°$ because Menrva is now near the apex of motion. The most probable impact velocity is ∼10.5 km/s (Zahnle et al., 2003). We assume densities of 0.6 g/cm^3 and 0.9 g/cm^3 for the impactor and surface, respectively. The nominal 444 km diameter Menrva basin would then correspond to a 210 km diameter apparent crater made by a 45 km diameter comet. This impact releases 1.6×10^{31} ergs. The same scaling relations applied to the putative ∼1200 km diameter Hotei impact suggest an impactor of $d_i \sim 150$ km and an energy of order 6×10^{32} ergs. Of course the uncertainties in these energy estimates are very large, at least a factor of 2 for Menrva and much more than this for the imperfectly seen Hotei basin.

2.2. Menrva vs. the atmosphere

To illustrate what 1.6×10^{31} ergs can do, we can ask how warm Titan's current atmosphere would get if uniformly heated. Atmospheric heating can be approximated by

$$E_{at} = (M_{N_2} + 2M_{CH_4})\, C_p\, (T - T_0) \tag{5}$$

where $M_{N_2} = 8.8 \times 10^{21}$ g (1.4 bars) and $M_{CH_4} = 2.5 \times 10^{20}$ g (0.07 bars) represent the masses of nitrogen and methane in the atmosphere, $C_p = 1.0 \times 10^7$ ergs/g/K is the heat capacity of N_2 (methane's heat capacity per gram, a weak function of T, is about twice nitrogen's), and the temperature T is raised from the unperturbed temperature T_0. If all 1.6×10^{31} ergs went into E_{at}, the temperature T would rise to 260 K, within reach of water's melting point. In practice some energy is deeply buried, or promptly radiated to space, or escapes from Titan as high speed ejecta (although most of these will be swept up again by Titan with no net loss of energy), or is locked away in the gravitational potential energy associated with impact-generated topography. Moreover, the atmosphere itself is more strongly heated aloft where most ejecta come to rest. Nevertheless we should expect the atmosphere as a whole to be heated considerably, and we should expect that a great deal of energy would be available to melt or evaporate surface volatiles. In consequence Titan's climate after Menrva will for some time be warmer and wetter than it is now.

Impacts somewhat bigger than Menrva — or Menrva itself if underestimated or taking place in a thinner atmosphere — are markedly more interesting, because they do lead to meltwaters at the surface. The purpose of this study is to provide a first

order descriptions of what probably happened after the Menrva impact, and of what may have happened after a putative Hotei impact.

3. Background assumptions

Titan is likely to have evolved significantly in response to *uv* photolysis, hydrogen escape, and the steady brightening of the Sun Lunine et al. (1989); McKay et al. (1993); Lorenz et al. (1997); McKay et al. (1999). At the currently observed hydrogen escape flux of 1.4×10^{10} H_2 molecules $cm^{-2}s^{-1}$ (referred to the surface, Ciu et al., 2008), Titan will consume its apparent methane inventories (Atreya et al., 2006; Lorenz et al., 2008) in 15-60 Myrs, depending on whether the chief product is ethane or H-poor polyaromatic hydrocarbons, respectively.

Another piece of the puzzle is that the products of billions of years of methane destruction are not visible on the surface (Le Gall et al., 2011). A representative photochemical model (Wilson and Atreya, 2004) predicts that ethane should accumulate at 40 m/Gyr. The observed H_2 escape flux implies a comparable accumulation rate for H-poor hydrocarbons. Le Gall et al. (2011) find that Titan's sand dunes today correspond to the equivalent of a global layer 0.6-6 m deep. At current rates, this layer would take 15-150 Myr to accumulate. Modeling of isotopic evolution of methane can be made consistent with an older age of 60-1600 Myr, but uncertainties in the modeling do not preclude 10 Myr (Nixon et al., 2012).

Taken together these observations — call them methane's time scale paradox — would seem to place us in a special time in Titan's history when methane is abundant. It is curious to note that crater counts and best estimates of the current impact cratering rate suggest that the surface itself may be older, some 200-1000 Myrs (Neish and Lorenz, 2012). For these reasons and others, Titan's story seems likely to have been complicated by non-uniformitarian tendencies.

Here we will set these worries aside and treat Titan at the times of big impacts as having an atmosphere and surface like today's and a crust made of water ice and methane. We restrict our consideration to three volatiles: N_2, H_2O, and CH_4. Our reasons for making these conservative assumptions are: (i) A nitrogen atmosphere like today's is a reasonable starting point, because the amount of N_2 outside Titan's interior is not likely to have changed greatly since Titan's formation (Mandt et al., 2009). The important qualification is that much or most of the nitrogen may have been in a condensed state similar to Triton when the Sun was fainter (McKay et al., 1999). (ii) Water ice is the default choice for the crust because water is almost certainly the most abundant ice in bulk Titan as it is generally in icy satellites (Soderblom et al., 2010). The simple morphology of Menrva suggests that Titan

had a relatively thick strong crust (Moore and Pappalardo, 2011). The important qualifications are that water ice is not unambiguously seen spectrally at the surface (Soderblom et al., 2010), and the rounded cobbles seen at the Huygens landing site may hint of something softer than water ice. (iii) Methane is currently the volatile that rains, and thus is the default agent of surface erosion. The important qualification is that methane may only be present in the atmosphere at special times. (iv) This is the first detailed study of its subject, and thus should be kept as simple as possible. The important qualification is that CO_2 ice (Wye et al., 2007), ethane (Lunine et al., 1989; Atreya et al., 2006), and several clathrates (Thomas et al., 2007, 2008; Mousis and Schmitt, 2008; Choukroun et al., 2010; Tobie et al., 2012) are all likely to be present or likely to form, and thus neglecting them may leave a system that is fundamentally too simple.

Our specific assumptions are an isothermal 1.4 bar N_2 atmosphere plus 5% CH_4, a water ice crust, and methane lakes that cover 3% of the surface to a depth of 40 m (equaling the 10^5 km^3 volume estimated by Lorenz et al., 2008). There is also methane in the soil. Heat from the Huygens Probe evaporated methane and other volatiles (including C_2H_6 and CO_2) from the surface (Niemann et al., 2005; Lorenz et al., 2006; Niemann et al., 2010), which suggests that the methane aquifer extends practically to the surface. We arbitrarily assume that the crust contains 5% methane [g/g], which corresponds to a porosity of 10% (liquid methane's density is about half that of the crust). We will assume that porosity extends to a depth $d_s = 1.5$ km as expected for ice in Titan's gravity. These assumptions correspond to a total crustal methane reservoir of 14×10^6 km^3 ($\sim$1.6 bars), which is big, about 24 times bigger than the atmospheric inventory. On the other hand, this volume of fluid falls short by a factor of $3 - 10$ of what is required to resolve the methane time scale paradox.

4. Model Details

We track the energy delivered by the impact as it flows through six reservoirs until Titan has returned to the state it was in before the impact came. The six reservoirs are the excess thermal energy in the atmosphere E_{at}; the excess thermal energy in the crust at temperatures below the melting point of water, E_{cr}; the latent heat associated with evaporating methane from the crust (E_{mvc}) and from lakes (E_{mvl}), $E_{mv} = E_{mvc} + E_{mvl}$; the latent heat associated with evaporating water from the crust, E_{wv}; the latent and sensible heats associated with melting and heating liquid water, E_{wl}; and the excess thermal energy associated with the water in an impact-generated crater lake, E_{cl}. Initial conditions are determined by iteratively solving the energy

equation as a function of environmental temperature T, written schematically

$$E = f_e E_i = E_{at}(T) + E_{cr}(T) + E_{mv}(T) + E_{wv}(T) + E_{wl}(T) + E_{cl}(T), \qquad (6)$$

where f_e represents the fraction of the impact's energy that would be available on time scales short enough to affect the climate. Subsequent evolution is determined by tracking the time rate of change of each of the six reservoirs, subject to the global boundary condition that Titan radiate the excess energy to space. For simplicity we assume that the surface and atmosphere are isothermal with temperature T, so that Titan radiates the impact energy as a blackbody at temperature T. The formal equation to describe cooling is

$$\begin{aligned} \frac{dE}{dt} &= -A\sigma\left(T^4 - T_0^4\right) \\ &= \frac{dE_{at}}{dt} + \frac{dE_{cr}}{dt} + \frac{dE_{mv}}{dt} + \frac{dE_{wv}}{dt} + \frac{dE_{wl}}{dt} + \frac{dE_{cl}}{dt}. \end{aligned} \qquad (7)$$

Titan's area is A. The σT_0^4 term takes into account insolation at the present albedo. The terms in Eqs (6) and (7) are described next.

4.1. Initial conditions

Most of the energy of the impact is initially invested in target materials close to where the comet strikes and in the materials of the comet itself. These materials are heated, melted, evaporated, and moved, such that many of the most strongly heated materials are ejected from the crater. A significant fraction of the kinetic energy is quickly shared with the atmosphere, through drag during ejection and then later, globally, when the more far-flung ejecta re-enter the atmosphere. Because the total mass ejected by Menrva would have been about a tenth that of the atmosphere as a whole, the atmosphere has the right scale to take up much of the energy initially in the impact ejecta.

Rather than fully model these events, we assume that a fraction f_e (usually 50%) of the impact energy goes into the atmosphere and the near surface environment. This energy includes almost all the kinetic energy in impact ejecta that escape from Titan, as the lost ejecta are mostly swept up again by Titan, where they will mostly heat the atmosphere or the near surface environment.

The fraction f_{cl} remains localized in the waters of the crater lake. Comparison to detailed computer models by Artemieva and Lunine (2005), Senft and Stewart (2011), and Kraus et al. (2011) imply that $f_{cl} \approx 0.1$. We find that very little of this energy is released quickly enough to affect the global climate. The rest of the impact energy, $1 - f_e - f_{cl}$, is presumed inaccessible, either deeply buried or lost through

radiative cooling from the top of the atmosphere when the bulk of the ejecta are first falling back to Titan and the upper atmosphere is both very hot and relatively opaque.

4.1.1. Atmosphere

For simplicity the atmosphere is presumed isothermal when heated, as described above by Eq (5). Atmospheric heating is a large term for Titan.

4.1.2. Crust

For the initial conditions we treat the crust, methane evaporated from the crust, meltwater, and water vapor as all coming out of the impact ejecta, and all in equilibrium with the atmosphere at a single temperature T. This approximation ignores, among other things, the likelihood that the impact-perturbed atmosphere will be hotter aloft than at the surface. It also ignores excavation and crustal heating associated with secondary craters, which are potentially considerable sources of readily-volatilized methane.

The mass of ejecta is approximated by

$$M_{\rm ej} = \rho_t V_{ap}. \tag{8}$$

We define E_{cr} as crustal heating to temperatures below the melting point,

$$E_{cr} = \begin{cases} M_{ej} C_v \left(T_m - T_0\right) & T > T_m \\ M_{ej} C_v \left(T - T_0\right) & T < T_m \end{cases} \tag{9}$$

where T_m is water's melting temperature and C_v is the heat capacity of the crust. For simplicity we have approximated $C_v = 1.3 \times 10^7$ ergs/g/K as the average of water ice's heat capacities at 90 K and 270 K.

We presume that all methane in the ejecta is liberated as vapor. The energy spent evaporating methane from the ejecta (crust) is

$$E_{mvc} = M_{ej} f_s L_v^{\rm CH_4}. \tag{10}$$

The mass of methane liberated from the crust is $E_{mvc} \div L_v^{\rm CH_4}$. The latent heat of condensation for methane is $L_v^{\rm CH_4} = 5.2 \times 10^9$ ergs/g. We assume that the crust (or soil) contains a uniform fraction $f_s = 0.05$ of methane [g/g], either to indefinite depth, or to a depth $d_s = 1.5$ km at which pores are squeezed shut.

If methane is in clathrate, the situation is more complicated but potentially more productive, as f_s can be as high as 0.13 in fully-loaded methane clathrate. At 1.5 bars, methane clathrate decomposes into methane gas and water ice at $T > 200$ K. For

Menrva, much or most of the ejecta get warm enough to meet this threshold, either directly through shock-heating or indirectly through interaction with the atmosphere. E.g., typical ejection velocities on the order $v_{ej} \sim \sqrt{Dg/2} \sim 0.5$ km/s imply heating of the same order of magnitude, $0.5 v_{ej}^2 \div C_v \sim 0.25 Dg \div C_v \sim 100$ K.

For very great impacts, there is energy enough to melt the ejecta

$$E_{wl} = \begin{cases} M_{ej} \left\{ L_m^{\mathrm{H_2O}} + C_v^{\mathrm{H_2O}} \left(T - T_m \right) \right\} & T > T_m \\ M_{ej} f_m L_m^{\mathrm{H_2O}} & T = T_m \\ 0.0 & T < T_m \end{cases} , \tag{11}$$

where f_m is the fraction of ejecta melted. The latent heat of fusion for water is $L_m^{\mathrm{H_2O}} = 3.3 \times 10^9$ ergs/g. The heat capacity of liquid water is $C_v^{\mathrm{H_2O}} = 4.2 \times 10^7$ ergs/g/K. The distinction between E_{cr} and E_{wl} drawn here is an arbitrary convenience for tracking liquid water.

The energy spent evaporating water is the biggest term for great impacts.

$$E_{wv} = M_{\mathrm{H_2O}} L_v^{\mathrm{H_2O}}, \tag{12}$$

where $M_{\mathrm{H_2O}}$ refers to the total mass of water vapor in the atmosphere,

$$M_{\mathrm{H_2O}} = \frac{p_{\mathrm{H_2O}}}{g} \frac{\mu_{\mathrm{H_2O}}}{\mu} A, \tag{13}$$

and $\mu_{\mathrm{H_2O}}$ and μ refer to the molecular weight of water and the mean molecular weight of the atmosphere, respectively. Water vapor is presumed saturated. The saturation vapor pressure is approximated by

$$p_{\mathrm{H_2O}} = p^*_{\mathrm{H_2O}} \exp\left(-T^*_{\mathrm{H_2O}} / T \right) \tag{14}$$

with $p^*_{\mathrm{H_2O}} = 5.46 \times 10^{11}$ dynes/cm^2 and $T^*_{\mathrm{H_2O}} = 5000$ K.

4.1.3. Ejecta heating of methane lakes

The amount of methane in the visible lakes is small compared to the amount of methane in the atmosphere. Lorenz et al. (2008) estimate that currently Titan's lakes have a volume on the order of 10^5 km^3, with an uncertainty of at least a factor of 3. This volume is equivalent to lakes with an average depth $d_L = 40$ m covering 3% of Titan's surface. When evaporated, the lakes add 0.01 bars of methane to the atmosphere. Methane lakes therefore do not play an important role in thermal evolution calculations made here.

Methane lakes are heated when struck by warm ejecta and methane will evaporate. The global average depth of the ejecta blanket is

$$d_{\rm ej} = \frac{M_{ej}}{\rho_t A}, \tag{15}$$

where A is Titan's area. Because the average is dominated by ejecta near the crater, the median may be more representative of conditions globally. We presume that the median is of the order $0.1 d_{ej}$. The excess thermal energy in the ejecta falling into the lake is presumed to evaporate methane (the kinetic energy is neglected). The depth of methane Δz_{ml} evaporated from the lakes is then

$$\Delta z_{ml} \rho_{ml} L_v^{\rm CH_4} = \begin{cases} 0.1\,\rho_{cr}\,d_{ej}\left(C_v\left(T_m - T_0\right) + L_m^{\rm H_2O} + C_v^{\rm H_2O}\left(T - T_m\right)\right) & T > T_m \\ 0.1\,\rho_{cr}\,d_{ej}\left(C_v\left(T_m - T_0\right) + f_m L_m^{\rm H_2O}\right) & T = T_m \\ 0.1\,\rho_{cr}\,d_{ej} C_v\left(T - T_0\right) & T < T_m \end{cases} \tag{16}$$

The corresponding energy in methane evaporated from lakes is

$$E_{mvl} = f_{ml} A \Delta z_{ml} \rho_{ml} L_v^{\rm CH_4}. \tag{17}$$

The mass of methane evaporated from lakes is $E_{mvl}/L_v^{\rm CH_4}$. The remnant of the lakes is left at the original temperature T_0. Ethane or propane in lakes is ignored.

4.1.4. The crater lake

Melt volumes computed by Artemieva and Lunine (2003, 2005), Kraus et al. (2011), and Senft and Stewart (2011) are in good agreement. Kraus et al. (2011) fit their computer model output with the empirical expression

$$\log_{10}\left(\frac{M_v + M_m}{m_i}\right) = a + 0.7\log_{10}\left(\cos\theta\right) - 0.46\phi + 1.5\left(\mu + 0.07\phi\right)\log_{10}\left(\frac{v_i^2}{E_M}\right), \tag{18}$$

in which M_m and M_v refer to melt and vapor volumes; m_i, v_i, and θ refer to the mass, velocity, and incidence angle of the impactor; ϕ refers to the porosity, $\mu = 0.554$, and $a = -0.36$ and $E_M = 8.2 \times 10^9$ ergs/g are nonunique fitting constants. The energy corresponding to the volume M_m of meltwater is

$$E_{cl} = f_{cl} E_i = M_m\left(C_v\left(T_m - T_0\right) + L_m^{\rm H_2O}\right). \tag{19}$$

We find that, for $v_i = 10.5$ km/s, $f_{cl} = 0.1$ provides a good match to M_m given by Eq (18).

The figures and supplemental on-line movies appended to Senft and Stewart (2011) suggest that more than 10% of the impact's energy is left buried in warm but

solid ice that envelopes the lake. The warm ice is likely a big term in the impact's energy budget. By assuming that 50% of the impact's energy goes into accessible energy and 10% into melt that remains in the crater, we implicitly assume that ∼40% of the impact's energy goes into warm ice. Little of this energy gets out of the crater quickly enough to affect the climate.

4.1.5. Initial conditions as a function of impact size

Figure 1 shows energy partitioning as a function of crater diameter. Two variants are shown, one in which ground-methane is confined to open pores in the uppermost $d_s = 1.5$ km of crust, the other extends methane to indefinite depth. For Menrva-scale and smaller impacts, available energy goes chiefly into heating the atmosphere. For impacts bigger than Menrva, the additional available energy is invested chiefly in melting and vaporizing water ice from the crust.

Figure 2 shows initial pressures and temperatures as a function of crater diameter. For smaller impacts, the "crust temperature" in Figure 2 refers to the ejecta blanket, which is assumed to be at the same temperature as the air. For bigger impacts, "crust temperature" in Figure 2 still refers to the ejecta blanket, but here liquified and mixed with ice from the crust. Mixing is expected given that any ice or hydrocarbons not firmly fastened to the bedrock will float to the top of the water. The crude assumption here is that the water's average temperature is intermediate between that of the atmosphere and that of melting ice. The surface of the water is assumed to be at the temperature of the atmosphere.

A more complex model is unjustified given that we do not know the composition of Titan's crust at the surface, much less at depth. It is not likely to closely resemble pure water ice. It may contain abundant hydrocarbons, abundant CO_2 ice, ammonia, possibly abundant hydrocarbon and CO_2 clathrates, etc. (Soderblom et al., 2010). Any abundant substance more volatile that H_2O will greatly affect the initial conditions shown in Figures 1 and 2, as well as the subsequent evolution. For example, a CO_2-rich or ethane-rich crust can begin to evaporate (or melt) for impacts smaller than Menrva, and if the associated energy sink is considerable, the surface temperature may not reach the melting point of water even for very great impacts. By comparison, the factor two uncertainties associated with the relationship between impact energy and crater size or with how much of the impact's energy goes into the atmosphere and surface materials are relatively minor concerns.

4.2. Environmental evolution after the impact

Environmental evolution after the impact is determined by integrating Eq (7) numerically as a function of time, beginning from initial conditions determined above.

The individual terms are described below. There are two basic regimes to consider. Smaller events do not raise the surface temperature to the melting point. The effects are limited to heating the crust and evaporating methane. Impacts that are big enough to melt the surface (i.e., those for which the initial temperature $T(t = 0)$ is greater or equal to water's melting temperature T_m) create oceans that, at the bottom, melt their way down into the crust (the "Xanadu syndrome"), while at the top, freezing and then slowly cooling to the atmosphere through a floating ice lid.

4.2.1. Atmosphere

The atmosphere is treated in the same way in either case. Evolution of E_{at} is mostly a matter of falling temperatures, with the rise and fall of excess methane playing a small role.

$$\frac{dE_{at}}{dt} = \left(M_{\mathrm{N_2}} + 2M_{\mathrm{CH_4}}\right) C_p \frac{dT}{dt} + 2C_p \left(T - T_0\right) \frac{dM_{\mathrm{CH_4}}}{dt} \tag{20}$$

The total mass of methane $M_{\mathrm{CH_4}}$ in the atmosphere is the sum of the methane in the atmosphere before the impact and the methane liberated from the crust and evaporated from the lakes:

$$M_{\mathrm{CH_4}} = M_{\mathrm{CH_4}}(0) + \frac{E_{mv}}{L_v^{\mathrm{CH_4}}} \tag{21}$$

In general, $M_{\mathrm{CH_4}}$ increases while the environment remains warm, then decreases with further cooling as the excess methane condenses and rains out; this will be discussed in more detail in section 4.2.9 below. Water vapor's sensible heat has been left out of E_{at} as a relatively small term compared to its latent heat.

4.2.2. Water vapor and water rain

Water vapor is also treated in the same way in either case. The energy stored in water vapor is approximated by the energy required to vaporize it,

$$E_{wv} = M_{\mathrm{H_2O}} L_v^{\mathrm{H_2O}}. \tag{22}$$

Precipitation of water is described by

$$\frac{dE_{wv}}{dt} = -\frac{dM_{\mathrm{H_2O}}}{dt} L_v^{\mathrm{H_2O}}. \tag{23}$$

Water vapor is presumed to be saturated at all times. The latent heat energy in water vapor is a big term in the energy budget of the biggest impacts.

4.2.3. The crust for smaller impacts

The crust is treated differently depending on whether water ice melts. Thermal energy in the solid crust E_{cr} is crudely approximated as a step function thermal wave. The crust is heated to $T_{cr} = T < T_m$ to a characteristic depth $z_{cr} \approx \sqrt{\kappa t}$ determined by thermal conduction, where t is time and κ [cm^2/s] is the thermal diffusivity. The progress of the thermal wave is approximated by

$$\frac{dz_{cr}}{dt} = 0.5\sqrt{\kappa/t}. \tag{24}$$

The thermal diffusivity κ is the ratio of thermal conductivity k_{cr} of the crust to the heat capacity $\rho_{cr}C_v$. For simplicity we ignore the T dependences of C_v and k_{cr} and use average values of $C_v = 1.3 \times 10^7$ [ergs/g/K] and $k_{cr} = 3.5 \times 10^5$ [ergs/cm/s/K] between 90 K and 270 K. Where methane evaporates, the latent heat of condensation raises the effective heat capacity and is taken into account:

$$\kappa = \begin{cases} \dfrac{k_{cr}}{\rho_{cr}C_v} & \text{no } CH_4 \text{ evaporates} \\ \dfrac{k_{cr}\,(T - T_0)}{\rho_{cr}C_v\,(T - T_0) + \rho_{cr} f_s L_v^{CH_4}} & \text{all } CH_4 \text{ evaporates} \end{cases} \tag{25}$$

Crustal heating is assumed to be global. With these approximations

$$\frac{dE_{cr}}{dt} = (M_{ej}C_v + \rho_{cr}C_v A z_{cr})\,\frac{dT}{dt} + \rho_{cr}C_v A\,(T - T_0)\,\frac{dz_{cr}}{dt}. \tag{26}$$

If after the impact there is no global melt, Eq (26) is complete. If there had been global melt, Eq (26) describes heating of the solid crust beneath the meltwaters, with the clock starting when the meltwaters have fully frozen.

4.2.4. The crust and meltwaters for larger impacts: Part I

We ignore topography and treat the meltwater as a global sheet of water of uniform depth. In general, a meltwater ocean of depth z_w consists of a liquid layer of thickness z_{wl} under an ice lid of thickness z_{ic} ($z_w = z_{wl} + z_{ic}$). The initial thickness of the meltwater sheet is determined by the ejecta, $z_{wl}(t{=}0) = f_m d_{ej}$.

While the atmosphere and meltwater remain warmer than T_m, the meltwater is heated by the atmosphere and the crust below is heated by the water. The temperature of the meltwater is presumed to be the average of the air temperature and the melting point of ice, $T_{wl} = (T - T_m)/2$. Define the energy in meltwater, E_{wl}, as the sum of latent heat spent melting water, $L_m^{H_2O}$, plus the extra thermal energy in water

warmer than T_m. Then

$$\frac{dE_{wl}}{dt} = \begin{cases} \rho_w A L_m^{\mathrm{H_2O}} \dfrac{dz_{wl}}{dt} & T = T_m \\ \rho_w A C_v^{\mathrm{H_2O}} z_{wl} \dfrac{dT_{wl}}{dt} + \rho_w A \left(C_v^{\mathrm{H_2O}} \left(T_{wl} - T_m \right) + L_m^{\mathrm{H_2O}} \right) \dfrac{dz_{wl}}{dt} & T > T_m \end{cases} . \tag{27}$$

Thermal conduction gives the minimum rate that heat propagates into the crust, dz_{cr}/dt as given by Eq (24). We will soon show in section 4.2.5 that Rayleigh-Taylor instability in warm ice heated by conduction predicts a minimum propagation rate somewhat faster than Eq (24). What we have called the crust energy $E_{cr} = \rho_{cr} C_v A z_{cr} \left(T_{ml} - T_0 \right)$ is constant with $z_{cr} = z_w$. We ignore the thermal energy in the relatively thin layer of warm ice under the melt.

There are several other effects, most hard to quantify, that affect heat transfer between the melt and the environment. Liquid water can drain into cracks or into pores vacated by methane. The water that drains into the ice freezes in the ice, and thus transfers heat into the ice. This is an important term in the energy budget of terrestrial glaciers (Fowler, 2011). How quickly this happens depends on the permeability of the ice, which initially might be considerable but might rather quickly become very low as frozen water fills the cracks and pores and the warm ice anneals.

On Titan loose debris will float to the top of the water. The debris include water ice but also hydrocarbons which in general float on water. The ice can melt, and some of the hydrocarbons can melt; both are heat sinks. Less volatile hydrocarbons will collect on the water's surface and accumulate on shorelines like running shoes. What qualifies as loose debris depends on the depth of the water, because the hydrostatic lifting force exerted by the denser water goes as $\Delta \rho g z_w$, to be compared to the strength that holds less dense material fixed to the bedrock. Thus a deeper ocean raises more flotsam. Organic flotsam is intriguing in itself, of course, but flotsam also inserts a layer of insulation between the atmosphere and meltwater, which would slow the cooling rate.

4.2.5. Rayleigh Taylor instabilities at the bottom of the sea

Because it is denser than ice, liquid water on ice is at best only conditionally stable. A lower limit on how quickly water and ice mix is set by Rayleigh-Taylor instabilities. Following Chandrasekhar (1961, pp. 443*ff*), the R-T growth rate n [sec^{-1}] as a function of wavenumber k [cm^{-1}] for an inviscid denser fluid (ρ_2) on top of a viscous less dense fluid (ρ_1, kinematic viscosity ν_1) is

$$n^2 + 2k^2 \alpha_1 \nu_1 \, n + gk \left(\alpha_1 - \alpha_2 \right) = 0 \tag{28}$$

where $\alpha_1 \equiv \rho_1/(\rho_1 + \rho_2)$. Surface tension is included by Chandrasekhar but is omitted here. The fastest growing mode grows at the rate

$$n_{\max}^3 = \frac{g^2 \left(\alpha_2 - \alpha_1\right)^2}{8\alpha_1 \nu_1} \tag{29}$$

and the wavenumber that corresponds to this fastest growing mode is

$$k_{\max}^3 = \frac{g \left(\alpha_2 - \alpha_1\right)}{8\alpha_1^2 \nu_1^2}. \tag{30}$$

Characteristic timescales and distance scales are $n_{\max}^{-1}$ and $k_{\max}^{-1}$, respectively. For Titan and warm ice, the time scale for overturn is fast but the length scale is long. Using $\nu_1 = 10^{14}$ cm^{2}s^{-1}, $n_{\max}^{-1} \approx 2 \times 10^4$ sec (6 hours), but $k_{\max}^{-1} = 1.5 \times 10^9$ cm, the circumference of Titan.

Shorter waves grow more slowly. We can neglect n^2 in Eq (28) for wavelengths short compared to $k_{\max}^{-1}$ to obtain

$$n = \frac{g \left(\alpha_2 - \alpha_1\right)}{2k\alpha_1 \nu_1} = \frac{g\Delta\rho L}{2\rho_1 \nu_1}, \tag{31}$$

where $\Delta\rho \equiv \rho_2 - \rho_1$. Here the length scale $L = k^{-1}$ is probably best identified with the thickness of warm ice under the lake. Stevenson (1981) identifies L with the characteristic vertical length scale set by the temperature dependence of viscosity, which can be appropriate here as well. For a crater lake L is best identified with the depth of warm shock-heated ice, which numerical simulations by Senft and Stewart (2011) using the 5-phase EOS suggest extends to about 20% of the diameter of the crater.

For surface meltwaters on top of cold ice, a lower limit on L is the depth $\sqrt{\kappa t_{\rm rt}}$ to which the cold ice is heated by thermal conduction. The basal ice overturns on a characteristic timescale $t_{\rm rt} = \left(2\rho_1\nu_1/\sqrt{\kappa} g \Delta\rho\right)^{2/3}$ and the water therefore melts into bedrock ice at a rate

$$\left(\frac{dz_w}{dt}\right)_{\rm RT} \approx \left(\frac{g\Delta\rho}{2\rho_1\nu_1}\right)^{1/3} \kappa^{2/3}. \tag{32}$$

The viscosity of terrestrial glaciers is $\sim 2 \times 10^{14}$ cm^2/s at a typical mean annual temperature of -20 C (Fowler, 2011). Viscosity is sensitive to temperature; an approximation is

$$\nu_1 \approx 4 \times 10^{12} \exp\left(\frac{T - T_m}{5 \text{ [K]}}\right) \text{ cm}^2/\text{s}. \tag{33}$$

Figure 3 compares Rayleigh-Taylor instability growth times to thermal conduction for scales pertinent to Titan. The combination of thermal conduction and R-T growth rates cause the melting front to propagate into a cold ice bedrock at an effective constant velocity on the order of $(dz_w/dt)_{\rm RT} \leq 2$ m/year. This is slow, albeit faster than thermal conduction working alone. It is a lower limit because it omits drainage of meltwaters into the ice.

4.2.6. The crust and meltwaters for larger impacts: Part II

The above considerations lead us to consider two descriptions of how quickly warm waters melt bedrock ice. The lower limit is given by Eq (32). The upper limit in reality is probably set by some combination of permeability and dynamic strength of the bedrock and the pressure exerted by the ocean. To illustrate what happens when water and ice mix more quickly, we arbitrarily enhance the thermal diffusivity into the ice by a factor 1000,

$$\left(\frac{dz_w}{dt}\right)_{\rm max} = 1000 \left(\frac{dz_w}{dt}\right)_{\rm RT}. \tag{34}$$

Cases using both Eq (32) and Eq (34) are shown in the results. While the oceans remain fully liquid, Eq (27) applies.

4.2.7. The crust and meltwaters for larger impacts: Part III

After the atmosphere cools below the melting point, an ice lid of thickness z_{ic} forms on the melt, and cooling of the interior is controlled by thermal conduction through ice. From this point forward, while liquid water remains, it is at the melting point, and Eq (27) is superceded by

$$\frac{dE_{wl}}{dt} = A\rho_w L_m^{\rm H_2O} \frac{dz_{wl}}{dt}. \tag{35}$$

What we have called the crust's energy E_{cr} decreases as the ice lid grows and cools,

$$\frac{dE_{cr}}{dt} = A\rho_c C_v \left(T_m - T_0\right) \frac{dz_{cr}}{dt} - \frac{1}{2} A\rho_c C_v \left(T_m - T_0\right) \frac{dz_{ic}}{dt} - \frac{1}{2} A\rho_c C_v z_{ic} \frac{dT}{dt}. \tag{36}$$

The interior as a whole (the meltwater ocean and the underlying crust) cools by conduction through the ice lid

$$\frac{dE_{cr}}{dt} + \frac{dE_{wl}}{dt} = -k\frac{T_m - T}{z_{ic}}. \tag{37}$$

Growth of the ice lid and the progress of the thermal wave are related to the freezing of liquid water by

$$\frac{dz_{cr}}{dt} = \frac{dz_w}{dt} = \frac{dz_{wl}}{dt} + \frac{dz_{ic}}{dt}, \tag{38}$$

where dz_{cr}/dt is given by the relevant form of Eq (32). Cases using both Eq (32) and Eq (34) are shown in the results.

4.2.8. The crust and meltwaters for larger impacts: Part IV

After all liquid water has frozen, $E_{wl} = 0$. The thermal wave continues to progress into the deeper crust at the rate dz_{cr}/dt given by Eq (24). Then

$$\frac{dE_{cr}}{dt} = A\rho_c C_v \left(T_{in} - T_0\right) \frac{dz_{cr}}{dt} + A\rho_c C_v \left(z_{cr} - \frac{z_{ic}}{2}\right) \frac{dT_{in}}{dt} - \frac{1}{2} A\rho_c C_v z_{ic} \frac{dT}{dt}. \tag{39}$$

where $T_{cr} = T_{in} < T_m$ is the (assumed isothermal) temperature in the frozen crust below the ice lid, and z_{ic} is held constant to its value when the ocean froze. The crust cools to the atmosphere as

$$\frac{dE_{cr}}{dt} = -k \frac{T_{in} - T}{z_{ic}}. \tag{40}$$

While warm enough, the thermal wave will continue to vaporize CH_4 as it progresses.

4.2.9. Methane evaporating from the crust

We presume that methane in the crust is liberated to the atmosphere when the crust melts. For crust that does not melt, we consider two cases. As a standard case we assume that methane degasses to the atmosphere if its vapor pressure exceeds the sum of atmospheric and lithostatic pressures. As an upper bound we assume that methane degasses if its vapor pressure exceeds the partial pressure of methane vapor in the atmosphere. In all three cases we assume that the liberated methane reaches the atmosphere rather than get caught in clathrates on its journey from the crust to the atmosphere. We will consider clathrates in Section 6.

The contribution to E_{mvc} from the crust is approximated by

$$\frac{dE_{mvc}}{dt} = \begin{cases} \rho_{cr} A f_s L_v^{\mathrm{CH_4}} \dfrac{dz_{cr}}{dt} & p_{cr} < p^*_{\mathrm{CH_4}}(T_{cr}) \text{ and } z_{cr} < d_s \\ 0 & p_{cr} > p^*_{\mathrm{CH_4}}(T_{cr}) \text{ or } z_{cr} > d_s. \end{cases} \tag{41}$$

The saturation vapor pressure of methane is approximated by

$$p^*_{\mathrm{CH_4}} = P^*_{\mathrm{CH_4}} \exp\left(-T^*_{\mathrm{CH_4}}/T\right) \tag{42}$$

where $P^*_{\rm CH_4} = 1.23 \times 10^{10}$ dynes/cm^2 and $T^*_{\rm CH_4} = 1050$ K. In our standard case the pressure p_{cr} is the lithostatic confining pressure

$$p_{cr} = z_{cr} g \rho_{cr} + p_{\rm atm}. \tag{43}$$

An upper limit to methane degassing assumes that crustal methane evaporates freely, so that $p_{cr} = p_{\rm CH_4}$. The pressure $p_{\rm CH_4}$ and mass $M_{\rm CH_4}$ are related by

$$p_{\rm CH_4} = \frac{M_{\rm CH_4}}{A} \frac{\mu}{\mu_{\rm CH_4}} g. \tag{44}$$

4.2.10. Methane evaporating from lakes

The contribution to E_{mv} from evaporating methane lakes, while they exist, is approximated by

$$\frac{dE_{mvl}}{dt} = \begin{cases} \rho_{ml} f_{ml} A L_v^{\rm CH_4} \dfrac{dz_{ml}}{dt} & p_{\rm CH_4} > p^*_{\rm CH_4}(T) \text{ and } z_{ml} < d_{ml} \\ 0 & p_{\rm CH_4} < p^*_{\rm CH_4}(T) \text{ or } z_{ml} = d_{ml} \end{cases} \tag{45}$$

Evaporation is a complicated problem. For Earth's lakes there are dozens of semi-empirical formulae to choose from Sartori (2000). One of the oldest and simplest is

$$\rho_{ml} L_v^{\rm CH_4} \frac{dz_{ml}}{dt} = h_e p_{at} \left(1 - \frac{p_{\rm CH_4}}{p^*_{\rm CH_4}} \right). \tag{46}$$

In Eq (46), the empirical heat transfer coefficient h_e is a velocity, $h_e = 3.6 + 0.025u$ [cm/s], in which u is the average wind velocity. The terms involving $p_{\rm CH_4}/p^*_{\rm CH_4}$ account for the humidity of the air. (Direct radiative heating by the atmosphere can be competitive with convective heating after great impacts, but under these conditions the lakes evaporate so quickly that there is no point in taking radiative heating into account.) For water and a typical terrestrial wind velocity of 400 cm/s, Eq (46) gives an evaporation rate of 5 mm/day, which is the accepted value for Earth.

How h_e should scale to Titan is not obvious. Factors at play must include the roughness of the lake's surface, the turbulence of the atmosphere near the surface, the innate bouyancy of the vapor, and the molecular diffusivity at the surface. Most of these should be smaller for unperturbed Titan than for Earth, which suggests that empirical coefficients derived for Earth and water are likelier to be too high than too small. Lorenz et al. (2012) compare predictions of two GCMs to estimate that winds over high latitude lakes are currently of order 500-1000 cm/s. The temperature difference between the atmosphere and the lake must be important when grossly out of equilibrium, as is the case after an impact. We might also expect a

more energetically circulating atmosphere and rougher lakes after an impact than at present. For specificity we leave the parameters in Eq (46) unchanged from Earth. In practice the lakes evaporate quickly under any assumptions and our results are insensitive to h_e.

4.2.11. Methane precipitating

When $p_{\rm CH_4} \leq p^*_{\rm CH_4}$, methane rains out, the energy stored in E_{mv} is returned as heat, and lakes and swamps refill with liquid methane,

$$\frac{dE_{mv}}{dt} = \begin{cases} 0 & p_{\rm CH_4} > p^*_{\rm CH_4}(T) \\ -\dfrac{dM_{\rm CH_4}}{dt} L_v^{\rm CH_4} & p_{\rm CH_4} \leq p^*_{\rm CH_4}(T) \end{cases} . \tag{47}$$

When raining, the atmosphere is presumed saturated with methane vapor.

4.2.12. Crater lakes: lifetimes and cooling rates

Artemieva and Lunine (2003, 2005) estimated melt volumes from detailed numerical simulations using the SOVA and SALEB hydrocodes and an ANEOS equation of state for water ice from Turtle and Pierazzo (2001). Two simulations were discussed in detail. A 35 km diameter crater produced a crater lake at the surface with a volume of ~ 50 km^3 of liquid water in an ~ 8 km diameter bowl. A 150 km diameter crater produced an annular crater lake 80 km across and as much as 5 km deep, with a volume $\sim 10^4$ km^3. Kraus et al. (2011) and Senft and Stewart (2011) obtain melt volumes that are essentially identical to those obtained by Artemieva and Lunine (2003, 2005) using the CTH hydrocode and their 5-phase EOS for water. Details are given for 2 km and 5 km diameter impacts. The 2 km impact generates a $\sim$35 km crater to be directly compared to the equivalent case discussed by Artemieva and Lunine (2003, 2005).

The lifetime of a crater lake at the surface would be long were its cooling controlled by thermal conduction through an ice lid (Thompson and Sagan, 1992; Artemieva and Lunine, 2005). In this case the cooling time would be $L_v^{\rm H_2O} h^2 / \left(k(T_m - T_s)\right)$, where h is the depth of the lake. A lake 1 km deep would last $\sim 20,000$ years. This is what one expects on Earth or Mars where a lake is set in rock (McKay and Davis, 1991)). But because liquid water is denser than ice, the lake is prone to overturning, and thus freezing more quickly.

Rayleigh-Taylor instabilities grow quickly when lakes are set in deep craters filled with warm ice. Senft and Stewart (2011) stress that their 5-phase EOS leaves a central plug of warm, $\sim$270 K, ice or slush. Although Senft and Stewart (2011) do not discuss whether crater lakes are left on the surface, their online supporting

movies clearly show liquid water sinking to the interface between cold ice at the bottom of the crater and the strongly shocked warm ice that fills the crater. This happens on a time scale of tens of minutes after impact. The ice is left with a low viscosity on a length scale comparable to the crater's depth. Figure 3 shows that, for any plausible viscosity, any lake in craters ranging from 35 km diameter to 1200 km overturns and mixes in less than a year — with the biggest, deepest lakes overturning in just a few days. What results therefore is not a lake but rather a plug of warm ice. This reinforces Senft and Stewart's results. Thus we conclude that crater lakes are probably short-lived on Titan. For the 35 km crater, if any liquid water remains, it ponds several kilometers below the surface. It is plausible that crater lakes, even the biggest, freeze very quickly.

On the other hand, the thermal energy buried in the crater is released too slowly to have a significant climatological impact. Figure 4 compares conductive and convective cooling time scales for warm ice. The conductive cooling time is

$$\tau_{\rm cond} = L^2/\kappa. \tag{48}$$

The convective cooling time is estimated using parameterized convection (Turcotte and Schubert, 1982),

$$\tau_{\rm conv} = Ra^{-1/3}/\kappa, \tag{49}$$

provided that the Rayleigh number

$$Ra = \frac{g\alpha\Delta T}{\nu\kappa L^3} \tag{50}$$

exceeds the critical Rayleigh number (657.5 for heating from below, Turcotte and Schubert, 1982). In these expressions $\alpha = 2\times10^{-4}$ (at 0 C) is the thermal expansivity; $\Delta T = T_{cl} - T$ is the temperature difference between the warm ice in the crater and the surface; and L, the depth of warm ice in the crater, can be approximated by the depth of the apparent crater. Figure 4 shows that cooling warm ice in a crater as big as Menrva would take at least ten thousand years.

5. Results

We begin with a Menrva-scale impact in Titan's current atmosphere. We then consider two impact sizes to span the range of what is plausible for the putative Hotei impact. The smaller impact releases 1.5×10^{32} ergs and corresponds to an 800 km crater on Titan. This impact energy is comparable to the Chicxulub event on Earth. The bigger impact releases 6×10^{32} ergs and generates a 1200 km diameter crater.

5.1. Menrva

Figure 5 addresses the energy budget and Figures 6 and 7 address crustal heating and the methane budget. All three show temperature. The nominal impact, which assumes that 50% of the impact energy goes into the atmosphere and ejecta, heats the atmosphere to 170 K. In the case where lithostatic pressure inhibits degassing (Figure 6), a few hundred millibars of methane geysers out of the upper 30 m of surface materials over a decade. In the case where crustal methane freely evaporates into the atmosphere, about twice as much methane reaches the atmosphere, taken from the upper 60 m of the crust. After $50 - 80$ years the atmosphere has cooled to the point that methane condenses and begins to drizzle out. Drizzling goes on for hundreds of years. Once the climate has returned to its pre-impact state, the new lakes are bigger than the old ones, with the extra methane having come out of the ground.

As an upper bound on Menrva, we consider a 30° (oblique) impact with $f_e = 0.8$. This gives a ∼450 km crater while putting a great deal of energy into the atmosphere and surface. Results are shown in Fig 8. The surface reaches 300 K. Water melts, evaporates, rains. The uppermost twenty meters or so of the crust melts and refreezes, surface methane triples, and the event as a whole lingers on for hundreds of years. It is possible that the consequences of these events, had they occurred, would still be visible on the surface.

5.2. 800 km (lesser) Hotei

Figures 9 and 10 respectively address the energy budget and the water and methane budgets for the lesser Hotei with basal melting given by Eq (32), which gives the slowest plausible rate for mixing heat into the interior, and thus gives the shallowest but longest-lasting liquid water seas. Most of the available energy goes into heating the atmosphere and melting and evaporating water. Heating the crust and evaporating methane are relatively unimportant (Fig. 9). The surface temperature reaches 350 K and remains above freezing for several years. Water vapor becomes abundant in the atmosphere. It rains. Open waters (Fig. 10) reach an average global depth of 50 m before they ice over. As the ocean freezes, the ice lid thickens while the remaining liquid water melts its way downward into the crust. The last meltwaters freeze 30 years after the impact at a depth of 140 m beneath new ice.

Ignoring possible clathration, methane would degas from the crust for 100 years from depths up to 200 m, putting about 0.2 bars of new methane into the atmosphere (Fig. 10). The methane later rains out over 1000 years to leave lakes of roughly 20× the volume of the current lakes. Atmospheric conditions approximate their pre-impact values after ∼1000 years.

Figures 11 and 12 assume that ice and water mix 1000× quickly, as given by Eq (34). Equation (34) minimizes the duration of liquid water but greatly enhances propagation of heat into the interior. This case is meant to parameterize the effects of cracks and porosity in the basement ice as conduits for falling water, flotation of loose debris, or any other shortcut to achieving a more stable density stratification. In this case open waters last three months and are 100 m deep and the last liquid water freezes nine months later at a depth of 300 m (Fig. 12). Crustal heating is the marked difference between the energy budgets shown in Figures 9 and 11. The more aggressive interior heating also mobilizes a great deal more methane. Together these effects cause the same 800 km impact to play out over a much longer period of time, of order 10^4 years rather than 10^3 years in the more conservative case.

5.3. 1200 km (greater) Hotei

Figures 13 and 14 present results for a 1200 km diameter greater "Hotei" with nominal and 1000×-enhanced thermal diffusivities in the ice under the meltwater seas. In both cases the global average surface temperature reaches 400 K after the impact and the energy budget after the impact (not shown) is dominated by water vapor.

In the nominal case (Fig. 13), open waters at the surface last for 40 years and the ocean fails to fully freeze until 200 years have passed; the last liquid water to freeze is under a lid of ice 600 m thick. Methane degassing is significant. It even plays a subtle role in the energy balance of the atmosphere, as methane evaporation in the warm crust and methane condensation in the cold atmosphere transfers enough energy from the interior to the atmosphere to warm the atmosphere (between 100 and 200 years).

In the 1000×-enhanced thermal diffusivity case, all methane that had been stored in the pores of the crust is released. This is why the partial pressure of atmosphere tops out in Fig. 14. This is a restatement of our assumption that methane in the crust is pore-filling and that the crust is not porous below 1.5 km. The enhanced thermal diffusion leads to a deep new ice crust, fully 1.7 km thick. At its greatest depth the open ocean was nominally 500 m deep. The hydrostatic pressure exerted by the ocean on the seafloor is plausibly great enough and applied long enough that it could rend the old cold crust apart and thrust sheets of water into the interior, rather than wait for viscosity to ooze ice out of the way. This provides an *a postiori* justification for artificially enhancing the thermal diffusivity.

6. Discussion: clathrates?

Clathrate hydrates are expected to be important in the outer solar system (Miller, 1961; Lewis, 1971). Titan is cold enough that methane clathrate hydrate is stable at the surface and through much of the crust (Lunine and Stevenson, 1987; Thomas et al., 2007; Choukroun et al., 2010; Tobie et al., 2012). Clathrate has been used by theorists to trap Kr and Xe (Thomas et al., 2008), noble gases that have not been seen in Titan's atmosphere (Niemann et al., 2005, 2010). The tentative measurement of a high $^{22}Ne/^{36}Ar$ ratio in the atmosphere (Niemann et al., 2010) also suggests a role for clathrates, because Ar can be trapped in ordinary clathrates but Ne cannot. Clathrates may also play a role in limiting the flow of radiogenic ^{40}Ar to the atmosphere.

On the other hand, there is no obvious evidence that clathrates interact with the present atmosphere. There is far too much methane in the atmosphere today (by a factor greater than a million) for it to be equilibrated with clathrates, and the CH_4/N_2 ratio is too high by orders of magnitude. The presence of methane lakes and damp ground at the surface also suggest that kinetic inhibition is the rule.

Methane clathrate forms readily in cold liquid water at pressures exceeding ~ 26 bars, but formation in crystalline ice is very slow and involves several steps (Kuhs et al., 2006). Currently available information is uncertain by orders of magnitude. For illustration we take Arrhenius coefficients from two recent studies to estimate reaction time scales pertinent to Titan. From Kuhs et al. (2006), we take their preferred activation evergy of 52 kJ/mole and a measured uptake of 6×10^{-7} moles/m^2/s for H_2O and CH_4 at 245 K and 60 bars, which imply a rate $k_1 = 8 \times 10^4 e^{-6300/T}$ moles/m^2/s. From Gainey and Elwood Madden (2012), we take their preferred activation evergy of 36 kJ/mole and a measured uptake of 2×10^{-5} moles/m^2/s at 250 K and 29 bars, which imply $k_2 = 1 \times 10^3 e^{-4400/T}$ moles/m^2/s. The two rates differ by two orders of magnitude, with k_1 being the slower. Both studies imply (over a small range of pressures) that rates go as p^2.

To estimate order-of-magnitude reaction times, we consider how long it would take for ice to consume Titan's current atmospheric methane inventory of 20 moles/m^2. Following Kuhs et al. (2006), we get

$$\tau_1 = 8 \times 10^{-8} \left(60/p\right)^2 \exp\left(6300/T\right) \text{ years.} \tag{51}$$

Following Gainey and Elwood Madden (2012), we get

$$\tau_2 = 7 \times 10^{-6} \left(30/p\right)^2 \exp\left(4400/T\right) \text{ years.} \tag{52}$$

These expressions imply that the atmosphere is stable against clathration for 10^{16} and 10^{25} years at 94 K, a degree of noninteraction that is equivalent to never.

Figures 15 and 16 compare the faster reaction time scale of Eq (52) to clathrate stability and to cooling after a greater Hotei impact. These calculations suggest that kinetics do not favor pure methane clathrate unless the depth of formation is greater than about a kilometer. The important exception would be in a crater lake where cooling time scales are much longer (Fig. 4).

Not all clathrates form as slowly as methane hydrate. For example, Pietrass et al. (1995) report that Xe clathrate forms in "tens of minutes" at ∼1 bar at 217 K and 195 K. Ethane clathrate is less stable than Xe but much more stable than methane clathrate. It is reasonable to expect ethane clathrate to form more quickly in cold ice than does methane clathrate.

If a clathrate forms, any other eligible gas may enter it in proportion to its relative abundance and in inverse proportion to its binary clathrate's decomposition pressure (Miller, 1961). The kinetics would then be those of the fastest-reacting abundant gas. Xenon itself despite its magnificent clathratibility is an unlikely candidate as a helping gas, but Titan has in ethane a plausible candidate for the role. Ethane has long been expected to be an abundant product of methane photolysis (Lunine et al., 1983). At 230 K, the ratio of their decomposition pressures is ten, so that a methane/ethane ratio of 10 in the gas phase would map to a clathrate with as much methane as ethane. In practice this means that clathrates would store ethane in preference to methane by a large factor, which is not in discord with the observed abundances of the two substances on Titan.

Figure 16 suggests that the cryptic clathrate layer formed by a greater Hotei-scale impact could easily be more than a kilometer thick. A kilometer of clathrate can contain the equivalent of 300 m of liquid methane, which exceeds the apparent surface reservoir by a factor of ~ 30 and would go a long way toward resolving methane's side of the time scale paradox. The clathrate can be exposed subsequently by erosion and other landscaping processes. Although methane clathrate is physically stable on Titan's surface today, its stability is questionable after global heating by a Menrva-scale impact, and its long-term stability with respect to weathering is at least worth raising as a question. If so, the erosion and degradation of methane clathrate could provide a continuing source of new methane to Titan's lakes and atmosphere, and the starting point of a plausible story for why Titan's soils are damp.

7. Summary

We have studied the thermal consequences of very big impacts on Titan. The approach adopted here is to follow three players: the energy, the methane, and of course the water. We assume that half of the impact energy is immediately available

to the atmosphere and surface while the other half is buried at the site of the crater and is unavailable on time scales of interest. The atmosphere and surface are treated as isothermal. We make the simplifying assumptions that the crust is everywhere as methane saturated as it was at the Huygens landing site, that the concentration of methane in the regolith is the same as it is at the surface, and that the crust is made of water ice. Heat flow into and out of the crust is approximated by step-functions. If the impact is great enough, ice melts. The meltwater oceans cool to the atmosphere conductively through an ice lid while at the base melting their way into the interior, driven down in part through Rayleigh-Taylor instabilities between the dense water and the warm ice. Topography, CO_2, and hydrocarbons other than methane are ignored. Methane and ethane clathrate hydrates are discussed quantitatively but not fully incorporated into the model. The interesting initial condition of nitrogen being condensed on a cold high albedo surface — a Triton-like Titan — is mentioned only in the summary.

We find that a nominal Menrva impact would have been big enough to raise the surface temperature by ∼80 K. Nominal Menrva would have doubled the methane inventory at the surface. The mobilized methane would have drizzled out of the atmosphere over hundreds of years, filling lake beds. Uncertainties in the impact energy and the partitioning of the energy into the atmosphere correspond to a factor two uncertainty in the temperature rise. Menrva was probably not big enough to heat the 1.4 bar N_2 atmosphere to the melting point of water, but some global-distributed surface melting cannot be ruled out at the high end of the uncertainty.

Hotei-scale impacts are more invigorating. If Titan's surface is mostly made of water ice, the putative Hotei impact raises the average surface temperature to between 350 and 400 K. Water rain must fall, flow, and pool in global meltwaters hundreds of meters deep. Meltwaters would have been subject to topographic control, flowing downhill and ponding, and subject to choking and crusting over with flotsam, the later including a variety of hydrocarbons, some of them liquid. When it finally fully freezes the ocean would be on the order of a kilometer deep. Global meltwaters may not endure more than a few decades or centuries at most, but are interesting to consider given Titan's organic wealth.

Clathrate hydrates might form under some of the conditions discussed here. Unfavorable kinetics would seem to restrict formation of the binary methane hydrate to depths greater than ∼1 kilometer of ice. Nonetheless it appears likely that methane migrating from below could have been caught in clathrates between 1 and 2 km depth, with capacity to store one to two orders of magnitude more methane than is currently in the atmosphere. Ethane hydrate has better prospects. Even if the kinetics are no faster for ethane than methane, ethane hydrate should have formed at

depths greater than 300 m. If the kinetics are more favorable, they would likely have formed within 100 m of the surface; if the kinetics are as favorable as they are for Xe, ethane clathrate would have formed at the surface. Any clathrate once formed can incorporate methane. Hence a kilometer of ethane clathrate can hold a great deal of methane. Whether decomposition of near-surface clathrates plays a part in resolving Titan's methane paradox is an open question, but it does seem plausible that near-surface clathrates can exist. We note that a near-surface clathrate source has inherent potential to provide a negative feedback that would keep the soil damp to the surface on longer timescales.

Impacts also create local crater lakes but, in disagreement with previous studies, we conclude that the lakes are likely to be deeply buried and very short-lived. The problem is that liquid water is denser than ice. Crater lakes form in shock-heated warm ice of relatively low viscosity. Rayleigh-Taylor instabilities in the warm ice grow quickly, the lakes founder, and the water mixes with ice. Any liquid water that remains unfrozen sinks to the bottom of the crater where it either pools kilometers below the surface in contact with cold bedrock ice. These concerns are general for any large icy satellite and not particular to Titan.

Hotei scale events, regardless of whether Hotei is itself a real exemplar, must have played a role in the history of Titan, as it is not plausible to build a world as big as Titan and not have big impacts. Thus the freeze-thaw cycle of Titan's surface water must have played some part in Titan's history.

Acknowledgments

The authors thank the NASA Cassini Data Analysis Program and the NASA Outer Planets Research Program for support of this work.

References

References

Artemieva, N., Lunine, J.I., 2003. Cratering on Titan: impact melt, ejecta, and the fate of surface organics. Icarus 164, 471–480.

Artemieva, N., Lunine, J.I., 2005. Impact cratering on Titan II. Global melt, escaping ejecta, and aqueous alteration of surface organics. Icarus 175, 522–533.

Atreya, S.K., Adam, E.Y., Niemann, H.B., Demick-Montelara, J.E., Owen, T.C., Fulchignoni, M., Ferrie, F., Wilson, E.W., 2006. Titan's methane cycle. Planet. Space Sci. 54, 1177–1187.

Atreya, S.K., Donahue, T.M., and Kuhn, W.R., 1978. Evolution of a nitrogen atmosphere on Titan. Science 201, 611–613.

Bronowski, J., 1973. The Ascent of Man. Little Brown, New York.

Chandrasekhar, S., 1961. Hydrodynamic and Hydromagnetic Stability. Dover, New York.

Chastain, B.K., Chevrier, V., 2007. Methane clathrate hydrates as a potential source for martian atmospheric methane. Planet. Space Sci. 55, 1246–1256.

Choukroun, M., Grasset, O., Tobie, G., Sotin, C., 2010. Stability of methane clathrate hydrates under pressure: Influence on outgassing processes of methane on Titan. Icarus 205, 581–593.

Cui, J., Yelle, R.V., Volk, K., 2008. Distribution and escape of molecular hydrogen in Titan's thermosphere and exosphere. J. Geophys. Res. 113, E10004.

Dones, L., Chapman, C.R., McKinnon, W.B., Melosh, H.J., Kirchoff, M.R., Neukum, G., Zahnle, K.J., 2009. Icy satellites of Saturn: Impact cratering and age determination. in: Dougherty, M., Bagenol, F., McKinnon, W.B. (Eds.), Saturn from Cassini-Huygens. Springer, Hamburg, pp. 613–635.

Fowler, A., 2011. Mathematical Geoscience. Series: Interdisciplinary Applied Mathematics, Vol. 36. Springer, Hamburg.

Gainey, S.R., Elwood Madden, M.E., 2012. Kinetics of methane clathrate formation and dissociation under Mars relevant conditions. Icarus 218, 513–524.

Korycansky, D.G., Zahnle, K.J., 2011. Titan impacts and escape. Icarus 211, 707–721.

Kraus, R.G., Senft, L.E., Stewart, S.T., 2011. Impacts onto H_2O ice: Scaling laws for melting, vaporization, excavation, and final crater size. Icarus 214, 724–738.

Kuhs, W.F., Staykova, D.K., Salamatin, A.N., 2006. Formation of methane hydrate from polydisperse ice powders. J. Phys. Chem. B. 110, 13283–13295.

Le Gall, A., Janssen, M.A., Wye, L.C., Hayes, A.G., Radebaugh, J., Savage, C., Zebker, H., Lorenz, R.D., Lunine, J.I., Kirk, R.L., Lopes, R.M.C., Wall, S., Callahan, P., Stofan, E.R., Farr, T., the Cassini Radar Team, 2011. Cassini SAR, radiometry, scatterometry and altimetry observations of Titan's dune fields. Icarus 213, 608–624.

Lewis, J.S., 1971. Satellites of the outer planets: their physical and chemical nature. Icarus 15, 174–185.

Lorenz, R.D., McKay, C.P., Lunine, J.I., 1997. Photochemically driven collapse of Titan's atmosphere. Science 275, 642–644.

Lorenz, R.D., Niemann, H.B., Harpold, D.N., Way, S.H., Zarnecki, J.C., 2006. Titan's damp ground: Constraints on Titan surface thermal properties from the temperature evolution of the Huygens GCMS inlet. Meteoritics Planet. Sci. 41, 1705–1714.

Lorenz, R.D., Mitchell, K.L., Kirk, R.L., Hayes, A.G., Aharonson, O., Zebker, H.A., Paillou, P., Radebaugh, J., Lunine, J.I., Janssen, M.A., Wall, S.D., Lopes, R.M., Stiles, B., Ostro, S., Mitri, G., Stofan, E.R., 2008. Titan's inventory of organic surface materials. Geophys. Res.Lett. 34, L07204.

Lorenz, R.D., Tokano, T., Newman, C.E., 2012. Winds and tides of Ligeia Mare, with application to the drift of the proposed time TiME (Titan Mare Explorer) capsule. Planet. Space Sci. 60, 72–85.

Lunine, J.I., Stevenson, D.J., Yung, Y.L., 1987. Ethane oceans on Titan. Science 222, 1229–1230.

Lunine, J.I., Stevenson, D.J., 1987. Clathrate and ammonia hydrates at high pressure: application to the origin of methane on Titan. Icarus 70, 61–77.

Lunine, J.I., Atreya, S.K., Pollack, J.B., 1989. Present state and chemical evolution of the atmospheres of Titan, Triton, and Pluto. in: Atreya, S.K., Pollack, J.B., Matthews, M.S. (Eds.), Origin and Evolution of Planetary and Satellite Atmospheres. University of Arizona Press, Tucson AZ, pp. 605–665.

Mandt, K.E., Waite, J.H., Lewis, W., Magee, B.A., Bell, J., Lunine J.I., Mousis, O., and Cordier, D., 2009. Isotopic evolution of the major constituents of Titan's atmosphere based on Cassini data. Planet. Space Sci. 57, 1917–1931.

McKay, C.P., Davis, W., 1991. Duration of liquid water habitats on early Mars. Icarus 90, 214–221.

McKay, C.P., Pollack, J.B., Lunine, J.I., Courtin, R., 1993. Coupled atmosphere-ocean models of Titan's past. Icarus 102, 88–98.

McKay, C.P., Lorenz, R.D., Lunine, J.I., 1999. Analytic solutions for the antigreenhouse effect: Titan and the early Earth. Icarus 137, 56–61.

Melosh, H.J., 1989. Impact Cratering: A Geological Process. Oxford Univ. Press, New York.

Melosh, H.J., Schneider, N.S., Zahnle, K.J., Latham, D., 1990. Ignition of global wildfires at the Cretaceous/Tertiary boundary. Nature 343, 251–254.

Miller, S.L. (1961). The occurrence of gas hydrates in the Solar System. Proc. Nat. Acad. Sci. 47, 1798–1808.

Moore, J.M., Pappalardo, R.T., 2011. Titan: an exogenic world? Icarus 212, 790–806.

Mousis, O., Schmitt, B., 2008. Sequestration of ethane in the cryovolcanic subsurface of Titan. Astrophys. J. 677, L67–L70.

Neish, C.D., Lorenz, R.D., 2012. Titan's global crater population: A new assessment. Planet. Space Sci. 60, 26–33.

Niemann, H.B., Atreya, S.K., Bauer, S.J., Carignan, G.R., Demiock, J.E., Frost, R.L., Gautier, D., Haberman, J.A., Harpold D.N., Hunten D.M., Israel, G., Lunine, J.I., Kasprzak, W.T., Owen, T.C., Paulkovich, M., Raulin, F., Way, S.H., 2005. The abundances of constituents of Titan's atmosphere from the GCMS instrument on the Huygens probe. Nature 438, 779—784.

Niemann, H.B., Atreya, S.K., Demick, J.E., Gautier, D., Haberman, J.A., Harpold, D.N., Kasprzak, W.T., Lunine, J.I., Owen, T.C., Raulin, F., 2010. Composition of Titan's lower atmosphere and simple surface volatiles as measured by the Cassini-Huygens probe gas chromatograph mass spectrometer experiment. J. Geophys. Res., 115, E12006.

Nisbet, E.G., Zahnle, K.J., Gerasimov, M.V., Helbert, J., Jaumann, R., Hofmann, B.A., Benzerara K., Westall, F., 2007. Creating habitable zones, at all scales, from planets to mud micro-habitats, on Earth and on Mars. Space Sci. Rev. 129, 79–121.

Nixon, C.A., Temelso, B., Vinatier, S., Teanby, N.A., Bézard, B., Achterberg, R.K., Mandt, K.E., Sherrill, C.D., Irwin, P.G.J., Jennings, DE, Romani, P.N., Coustenis, A., and Flasar, F.M., 2012. Isotopic ratios in Titan's methane: measurements and modeling. Astrophys. J. 749, 159 (15pp).

O'Brien, D.P., Lorenz, R.D., Lunine, J.I., 2005. Numerical calculations of the longevity of impact oases on Titan. Icarus 173, 243–253.

Pietrass, T., Gaede, H.C., Bifone, A., Pines, A., Ripmeester, J.A., 1995. Monitoring xenon clathrate formation on ice surfaces with optically enhanced ^{129}Xe NMR. J. Amer. Inst. Chem. Soc. 117, 7520–7525.

Sartori, E., 2000. A critical review on equations employed for the calculation of the evaporation rate from free water surfaces. Solar Energy 68, 77–89.

Schmidt, R.M., Housen, K.R., 1987. Some recent advances in the scaling of impact and explosive cratering. Int. J. Impact Engineering 5, 543–560.

Segura, T.L., Toon, O.B., Colaprete, A., Zahnle, K.J., 2002. Environmental effects of large impacts on Mars. Science 298, 1977–1980.

Senft, L.E., Stewart, S.T., 2011. Modeling the morphological diversity of impact craters on icy satellites. Icarus 214, 67–81.

Sleep, N.H., Zahnle, K.J., Kasting, J.F., Morowitz, H., 1989. Annihilation of ecosystems by large asteroid impacts on the early Earth, Nature 342, 139–142.

Sleep, N.H., Zahnle, K.J., 1998. Refugia from Asteroid Impacts on Early Mars and the Early Earth. J. Geophys. Res. 103, 28529–28544.

Soderblom, L.A., Brown, R.H., Soderblom, J.M., Barnes, J.W., Kirk, R.L., Sotin, C., Jaumann, R., Mackinnon, D.J., Mackowski, D.W., Baines, K.H., Buratti, BJ, Clark, R.N., Nicholson, P.D., 2009. The geology of Hotei Regio, Titan: Correlation of Cassini VIMS and RADAR. Icarus 204, 610–618.

Soderblom, L.A., Barnes, J.W., Brown, R.H., Clark, R.N., Janssen, M.A., McCord, T.B., Niemann, H.B., Tomasko, M.G., 2010. Composition of Titan's surface. in: Brown, R.H., Lebreton, J.-P., Waite, J.H. (Eds.), Titan from Cassini-Huygens. Springer, Hamburg, pp. 141–176.

Staykova, D.K., Hansen, T., Salamatin, A.N., Kuhs, W.F., 2002. Kinetic diffraction experiments and the formation of porous gas hydrates. Proc. Fourth Int. Conf. on Gas Hydrates, pp 537–642.

Stevenson, D.J., 1981. Models of Earth's core. Science 214, 611–619.

Stevenson, D.J., Harris, A.W., Lunine, J.I., 1986. Origins of satellites, in: Burns, J.A., Mathews, M.S. (Eds.), Satellites. University of Arizona Press, Tucson AZ, pp. 39–88.

Thomas, C., Mousis, O., Ballenegger, V., Picaud, S., 2007. Clathrate hydrates as a sink of noble gases in Titan's atmosphere. Astron. Astrophys. 474, L17–L20.

Thomas, C., Picaud, S., Mousis, O., Ballenegger V., 2008. A theoretical investigation into the trapping of noble gases by clathrates on Titan. Planet. Space Sci. 56, 1607–1617.

Thompson, W.R., Sagan, C., 1992. Organic chemistry on Titan — surface interactions. in: Kaldeich, B. (Ed.), Proceedings of the Symposium on Titan. ESA SP, vol. 338. ESA, Noordwijk, the Netherlands, pp. 167–176.

Tobie, G., Lunine, J.I., Sotin, C., 2006. Episodic outgassing as the origin of atmospheric methane on Titan. Nature 440, 61–64.

Tobie, G., Gautier, D., Hersant, F., 2012. Titan's Bulk Composition Constrained by Cassini-Huygens: Implication for Internal Outgassing. Astrophys. Journal 752, 125 (10 pp.)

Turtle, E.P., Pierazzo, E., 2001. Constraints on the thickness of an Europan ice shell from impact crater simulations. Science 234, 1326–1328.

Turcotte, D.L., Schubert, G., 1982. Geodynamics. John Wiley, New York.

Voss, L.F., Henson, B.F., Robinson, J.M., 2007. Methane thermodynamics in nanoporous ice: A new methane reservoir on Titan. J. Geophys. 112, E05002.

Wilson, E.W., Atreya, S.K., 2004. Current state of modeling the photochemistry of Titan's mutually dependent atmosphere and ionosphere. J. Geophys. Res. 109, E06002.

Wood, C.A., Lorenz, R.D., Kirk, R.L., Lopes, R.M., Mitchell, K., Stofan, E., the Cassini RADAR Team, 2010. Impact craters on Titan. Icarus 206, 334–344.

Wye, L.C., Zebker, H.A., Ostro, S.J., West, R.D., Gim, Y., Lorenz, R.D., and the Cassini RADAR Team, 2007. Electrical properties of Titan's surface from Cassini RADAR scatterometer measurements. Icarus 188, 367–385.

Zahnle, K.J., 1990. Atmospheric chemistry by large impacts. in: Sharpton, V., Ward, P. (Eds.), Global Catastrophes in Earth History. GSA Special Paper 247, 271–288.

Zahnle, K.J. and Sleep, N.H., 1997. Impacts and the early evolution of life. in Thomas, P., Chyba, C., McKay, C.P. (Eds.), Comets and the Origin of Life. Springer-Verlag, Hamburg, pp. 175–208.

Zahnle, K.J., Schenk, P., Sobieszczyk, S., Dones, L., Levison, H., 2003. Cratering rates in the outer solar system. Icarus 163, 263–289.

Zahnle, K.J, Arndt, N., Cockell, C., Halliday, A.N., Nisbet, E.G., Selsis, F., Sleep, N.H., 2007. Emergence of a habitable planet. Space Sci. Rev. 129, 35–78.

Zahnle, K.J., Alvarellos, J.L., Dobrovolskis, A.R., Hamill, P., 2008. Secondary and sesquinary craters on Europa. Icarus 194, 660–674.

Figure Captions

Figure 1
Initial partitioning of impact energy as a function of crater diameter on Titan. Atmospheric heating is denoted E_{at}. Residual thermal energy in impact ejecta at temperatures less than the melting point of water is E_{cr} (or "crust"). Energy in water vapor (E_{wv}) is dominated by the latent heat of vaporization. Energy in liquid water (E_{wl}) is the sum of the latent heat of melting and the thermal energy of liquid water. Energy in methane (E_{mv}) refers to the latent heat of evaporated methane, mostly from the crust. In one case methane presumes 5% methane is present in the upper $d_s = 1.5$ km of the crust, the other presumes 5% methane is present at all depths. Not plotted are the energies of the crater lake and any heat that remains deeply buried in or near the crater.

Figure 2
Initial temperatures and pressures after an impact as a function of crater diameter. "Ocean temperature" refers to the average temperature of liquid water at the surface. Methane partial pressures include the methane already present in the atmosphere. The two methane cases are described in the caption to Fig. 1. Methane's saturation vapor pressure as a function of temperature is shown for comparison.

Figure 3
A comparison of cooling times of impact-generated Titanian lakes to Rayleigh-Taylor timescales for ice and water to overturn. "Freezing by conduction" refers to how quickly a lake freezes when cooling is limiting by conduction through an ice lid. "R-T growth" refers to growth of Rayleigh-Taylor instabilities in warm ice of the indicated viscosities. If the warm ice is thick, R-T instabilities grow very quickly and water and ice will at minimum interchange and, at maximum, mix to a slush. "Conductive cooling of basal ice" refers to thermal conduction of heat from the water into initially cold ice bedrock. The shading on the left indicates the regime in which R-T instabilities grow in conductively heated ice. The melting front propagates into cold ice bedrock at a rate of 30 to 60 m over 20 to 100 years. Although slow, this is faster than cooling through an ice lid. The regime pertinent to the craters themselves is indicated by the shading on the right. The depth of warm ice for a given crater is labeled by "crater size."

Figure 4
Conductive and convective cooling time scales of warm ice as a function of temperature (viscosity). For convection, the Rayleigh number increases from left to right

along an isotherm; the left limit is set by the critical Rayleigh number below which convection does not occur. It appears that deep warm ice — i.e., the material filling the bigger craters — should cool convectively, but on time scales that are long compared to the climatological effects discussed in the next section.

Figure 5
Cooling after a Menrva impact: the energy budget. The impact's energy is partitioned between heat in the atmosphere, heat in the ejecta and the crust, and evaporation of methane from lakes and from the ejecta and crust. The temperature of the surface and atmosphere are shown against the right-hand axis.

Figure 6
Cooling after a nominal Menrva impact: pressures and depths. "Crust heating depth" refers to how deeply the crust is heated by the thermal wave. This includes the nominal average thickness of the ejecta blanket, which is why the curve does not start at zero. Saturated and atmospheric methane vapor pressures are shown against the right-hand axis. This case assumes that methane is released to the atmosphere if the vapor pressure of methane in the crust exceeds the ambient lithostatic pressure. This is why p_{CH_4} tops out at 0.105 bars. The volume of methane lakes is given in bars (the partial pressure that would result by evaporating the lakes).

Figure 7
Cooling after a nominal Menrva impact. This case assumes that methane is released to the atmosphere if the vapor pressure of methane in the crust exceeds the partial pressure of methane in the atmosphere. More methane is released than in Fig. 6.

Figure 8
Cooling after a maximum Menrva impact. This case assumes a 30° (oblique) impact with 80% of the impact energy available for heating the atmosphere and surface. The depth of surface melt is indicated by the ice lid. Water vapor pressure is indicated. Ocean (and frozen ocean) temperature lags behind air temperature. Surface methane triples.

Figure 9
Cooling after a lesser (800 km crater) Hotei impact: the energy budget with nominal thermal diffusivity. "Crust" refers only to heating to temperatures below the melting point of water. Any melting and any extra heat in liquid water is accounted as liquid "liquid water." "Methane vapor" and "water vapor" refer only to energy invested in vaporization.

Figure 10
Cooling after a lesser (800 km crater) Hotei impact: pressures and depths with nominal thermal diffusivity. Conditions at the surface remain temperate for several years. "Ocean temperature" refers to the average temperature of the liquid water. The dotted curve denoted "ice lid" refers to the total depth of the ocean, which includes both the liquid water and the ice sheet floating on top. The total depth of the ocean increases linearly with time because of the combined effects of thermal conduction and the growth of Rayleigh-Taylor instability in the warm ice. The methane inventory at the surface triples.

Figure 11
The energy budget after a lesser (800 km crater) Hotei impact when thermal diffusivity in ice contiguous to liquid water is amplified 1000× (thermal diffusivity after all water has frozen is returned to its normal value). The purpose of raising thermal diffusivity is to enhance mixing of water and underlying ice. This assumption is meant to approximate what might happen if liquid waters flowed into cold fractured permeable bedrock ice, or if the oceans were choked with loose debris. Ice and water mix more quickly, the water freezes more quickly, and the impact energy is transported more deeply into the crust than in Fig 9. Hence more energy goes into crustal heating and methane vaporization than in Fig 9.

Figure 12
Cooling after a lesser (800 km crater) Hotei impact with 1000× enhanced thermal diffusitivity. Liquid water is deeper but shorter lived than in Fig 10 with nominal thermal diffusivity. The final frozen ice lid is almost 300 m thick. Toward the end of the event, methane released from the warm crust condenses directly upon entering the colder atmosphere, which is why there is more methane in lakes than the maximum seen in the atmosphere.

Figure 13
Cooling after a greater (1200 km diameter) Hotei impact with nominal thermal diffusivity. Results are qualitatively similar to those in Fig. 10, but amplified. The increase in methane vapor pressure between 100 and 200 years is caused by the atmosphere warming slightly by condensation of methane degassed from the warm crust.

Figure 14
Cooling after a greater (1200 km diameter) Hotei impact with 1000× enhanced thermal diffusivity. Results are qualitatively similar to those in Fig. 12, but amplified.

At its deepest the liquid water is more than 500 m deep. An ice lid forms at 200 years and thickens until the final frozen ocean is 1.7 km thick. If clathrate formation is ignored, the amount of methane at the surface is raised by a factor of 20.

Figure 15
Clathrates after the impact of Fig. 13. The upper panel compares estimated time scales for methane clathrate formation (Eq 52) to cooling times. The lower panel compares depths of clathrate stability (lithostatic pressure as a function of the temperature shown in the upper panel) to relevant hearing depths. Without a helping gas, the kinetics appear to be unfavorable and methane clathrate is unlikely to form at depths shallower than 1 km. Ethane clathrate would form readily as water freezes at depths below 300 m. If ethane clathrate forms as quickly in ice as Xe clathrate, ethane clathrates would form at the surface while temperatures were above 200 K.

Figure 16
Clathrates after the impact of Fig. 14. In this case the warm ice is thicker, the time scales longer, and the kinetics more favorable to clathrate formation. Under these conditions a considerable amount of methane could be trapped in clathrates one to two kilometers below the nominal surface. If ethane were abundant, clathrates would likely form within 100 meters of the nominal surface.

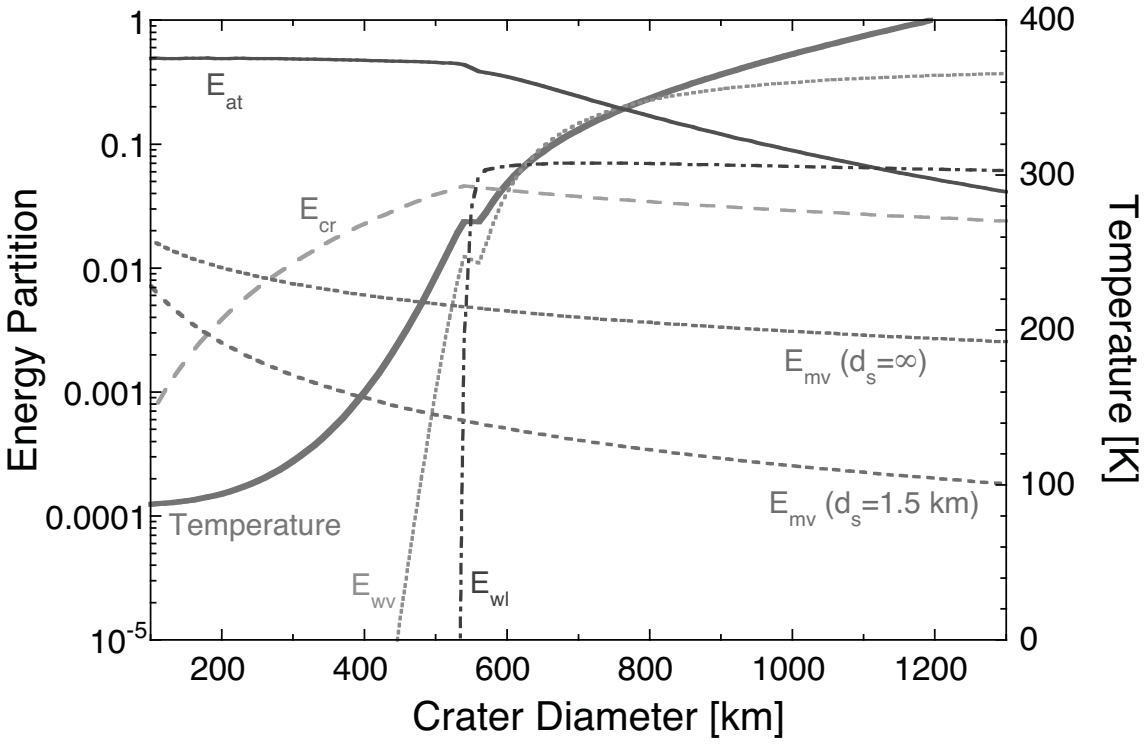
Energy Partition
Temperature [K]
Crater Diameter [km]
E_at
E_cr
E_mv (d_s=∞)
E_mv (d_s=1.5 km)
Temperature
E_wv
E_wl
1
0.1
0.01
0.001
0.0001
10^-5
400
300
200
100
0
200
400
600
800
1000
1200

Figure 1:

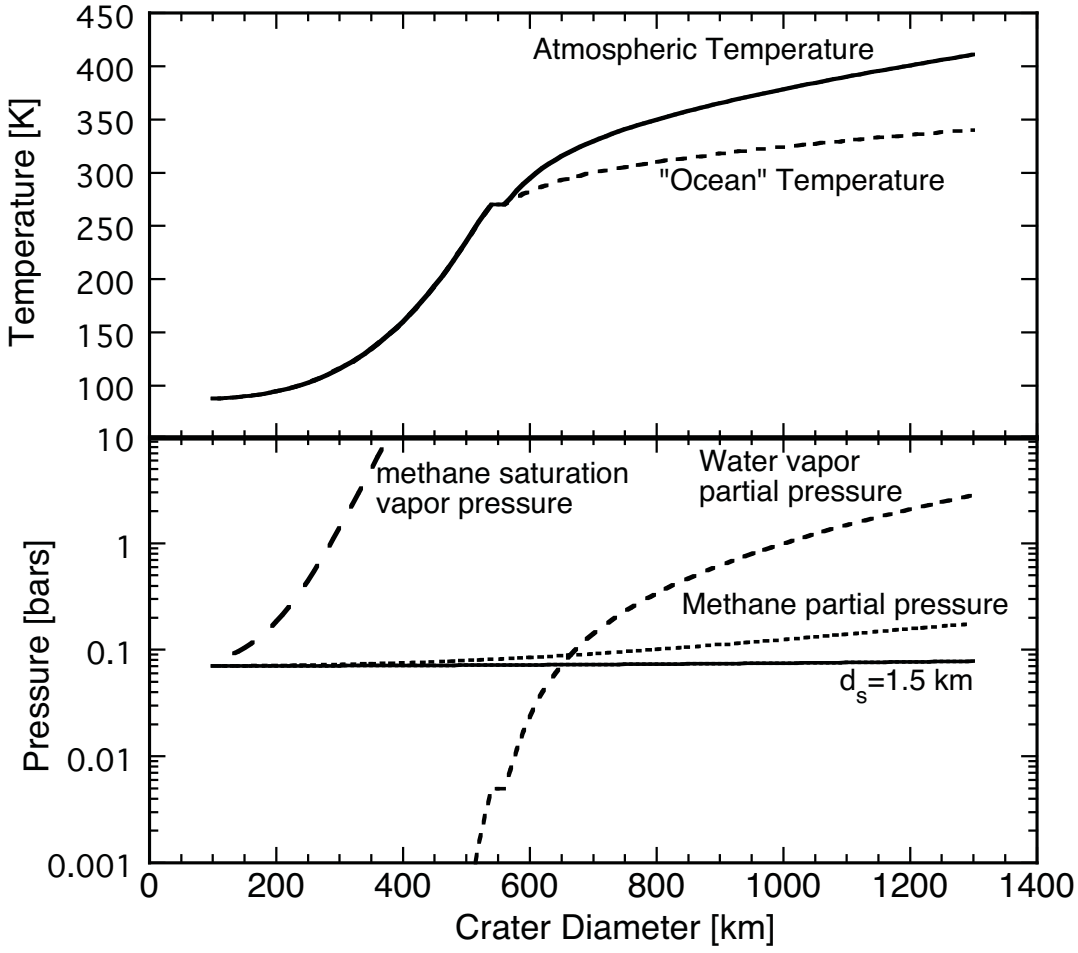
Atmospheric Temperature
"Ocean" Temperature
Temperature [K]
450
400
350
300
250
200
150
100
10
methane saturation
vapor pressure
Water vapor
partial pressure
Methane partial pressure
d_s=1.5 km
Pressure [bars]
1
0.1
0.01
0.001
0
200
400
600
800
1000
1200
1400
Crater Diameter [km]

Figure 2:

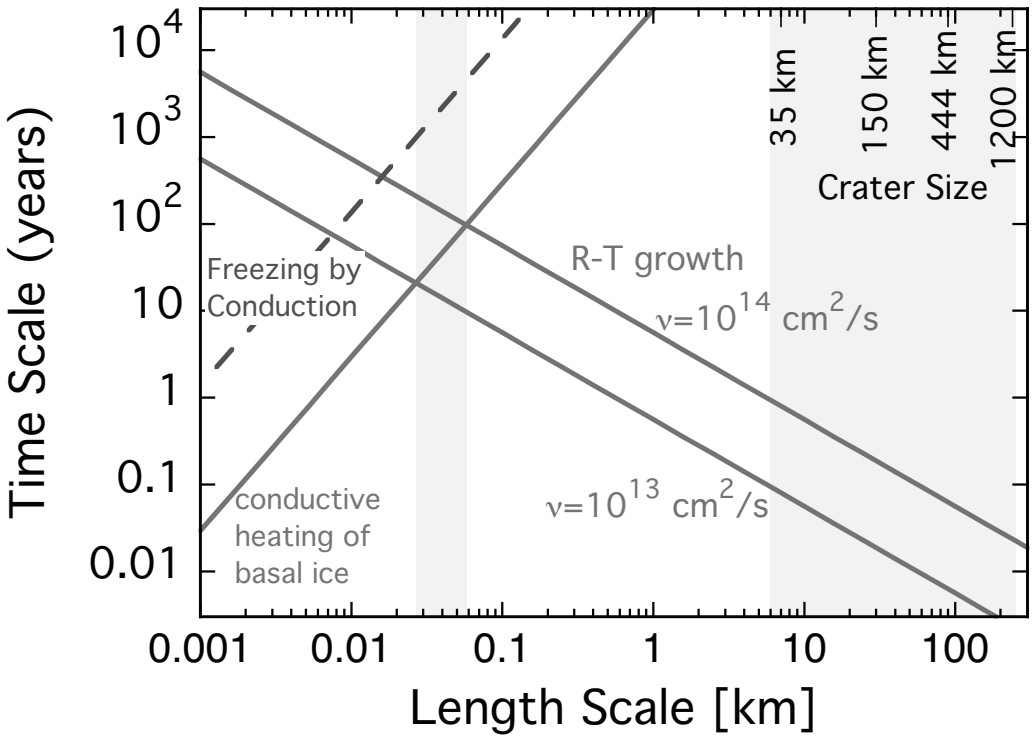
Time Scale (years)
Length Scale [km]
10^4
10^3
10^2
10
1
0.1
0.01
0.001
0.01
0.1
1
10
100
35 km
150 km
444 km
1200 km
Crater Size
R-T growth
ν=10^14 cm^2/s
ν=10^13 cm^2/s
Freezing by
Conduction
conductive
heating of
basal ice

Figure 3:

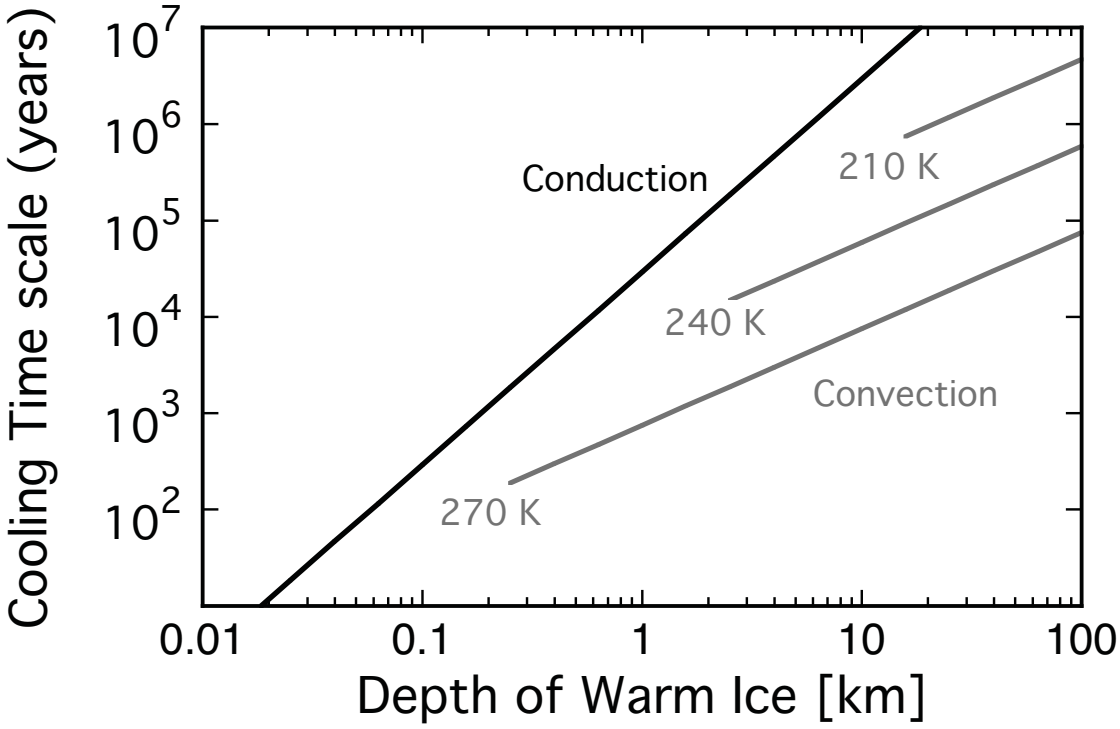
Cooling Time scale (years)
10^7
10^6
10^5
10^4
10^3
10^2
Conduction
210 K
240 K
Convection
270 K
0.01
0.1
1
10
100
Depth of Warm Ice [km]

Figure 4:

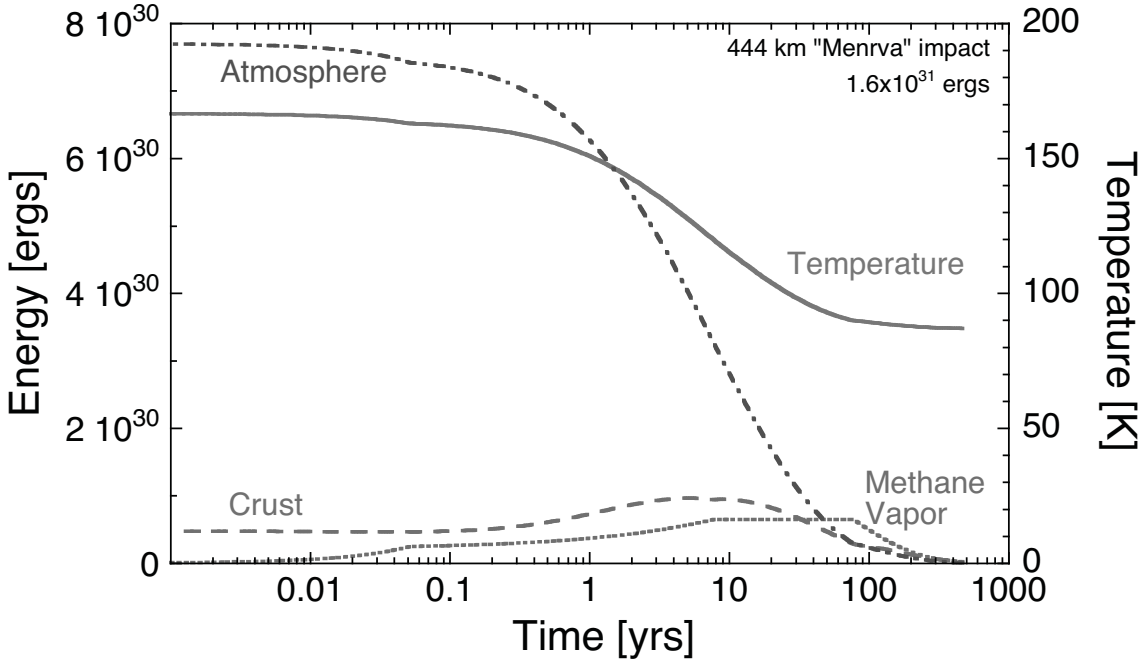
8 10^30
6 10^30
4 10^30
2 10^30
0
Energy [ergs]
200
150
100
50
0
Temperature [K]
444 km "Menrva" impact
1.6x10^31 ergs
Atmosphere
Temperature
Crust
Methane
Vapor
0.01
0.1
1
10
100
1000
Time [yrs]

Figure 5:

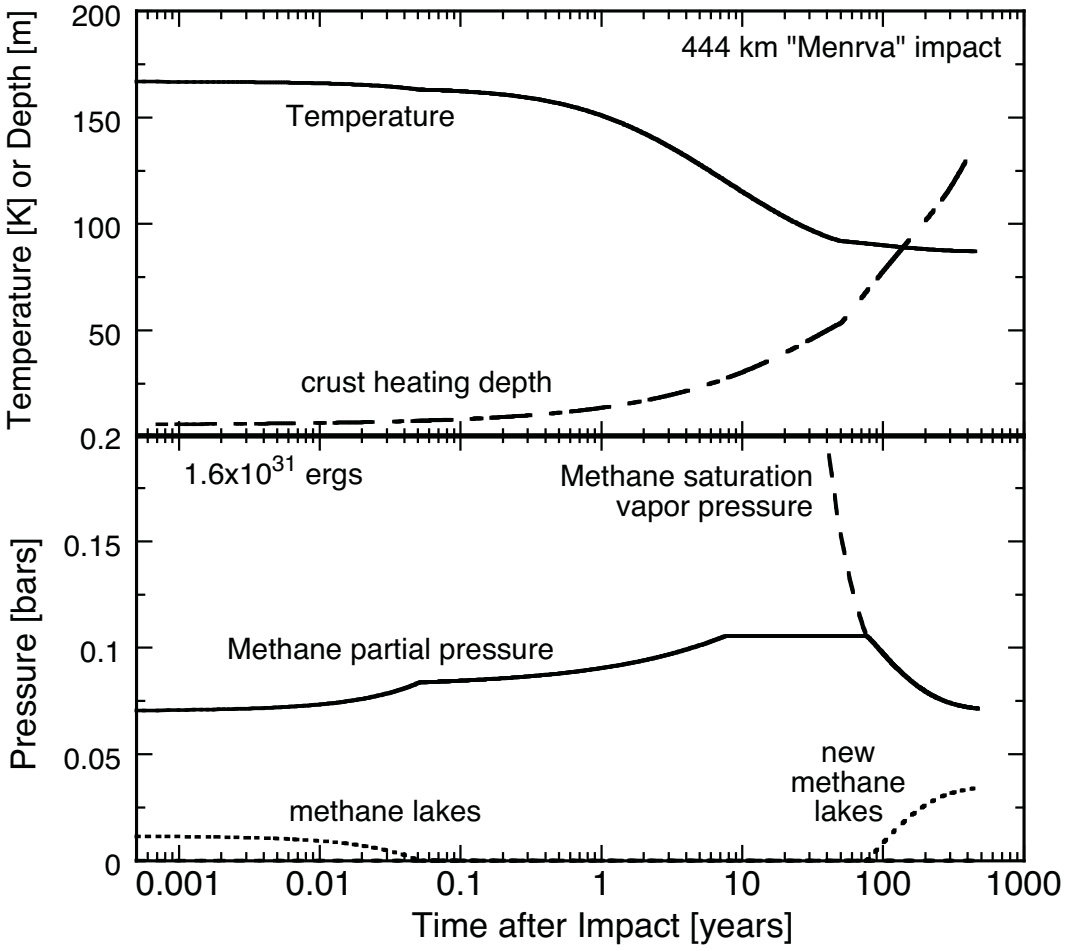
444 km "Menrva" impact
Temperature
crust heating depth
1.6x10^31 ergs
Methane saturation
vapor pressure
Methane partial pressure
methane lakes
new
methane
lakes
Temperature [K] or Depth [m]
Pressure [bars]
Time after Impact [years]
200
150
100
50
0.2
0.15
0.1
0.05
0
0.001
0.01
0.1
1
10
100
1000

Figure 6:

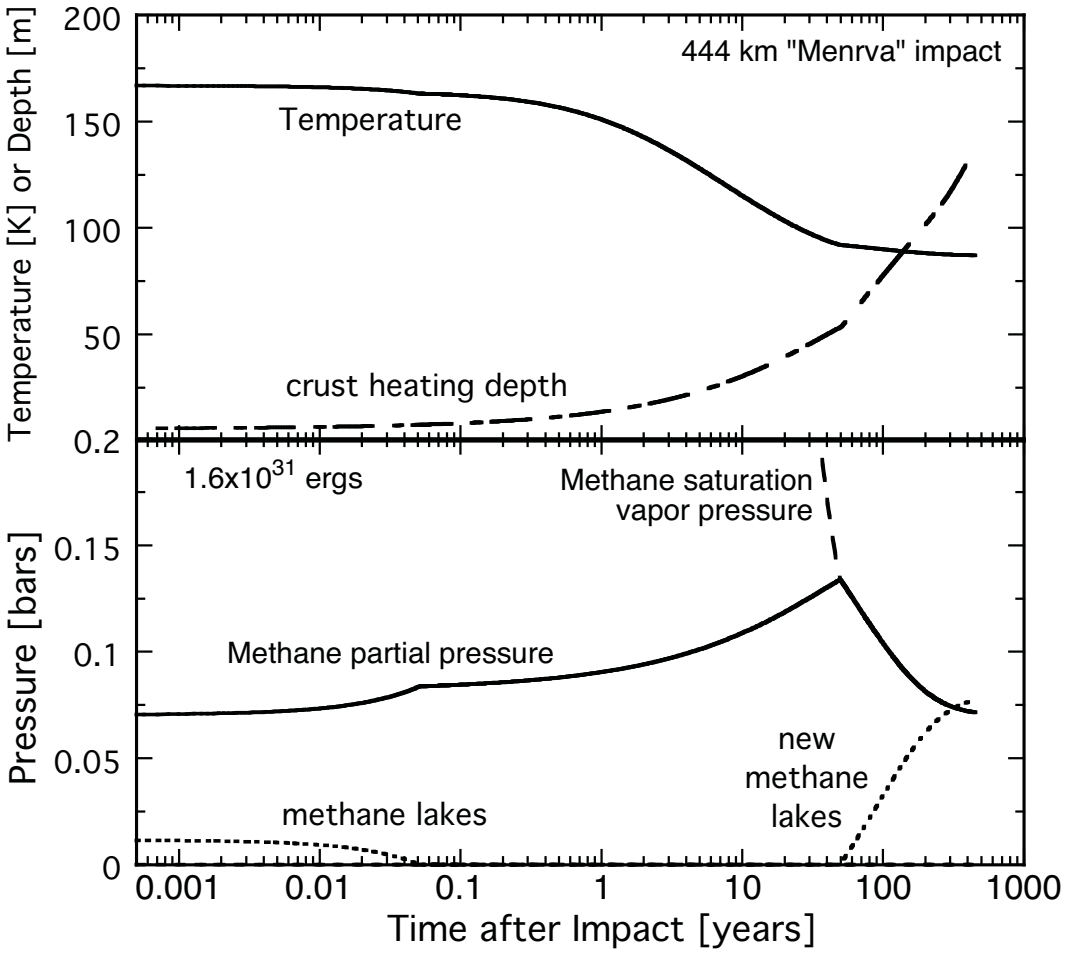
444 km "Menrva" impact
Temperature
crust heating depth
1.6x10^31 ergs
Methane saturation
vapor pressure
Methane partial pressure
new
methane
lakes
methane lakes
Temperature [K] or Depth [m]
Pressure [bars]
Time after Impact [years]
200
150
100
50
0.2
0.15
0.1
0.05
0
0.001
0.01
0.1
1
10
100
1000

Figure 7:

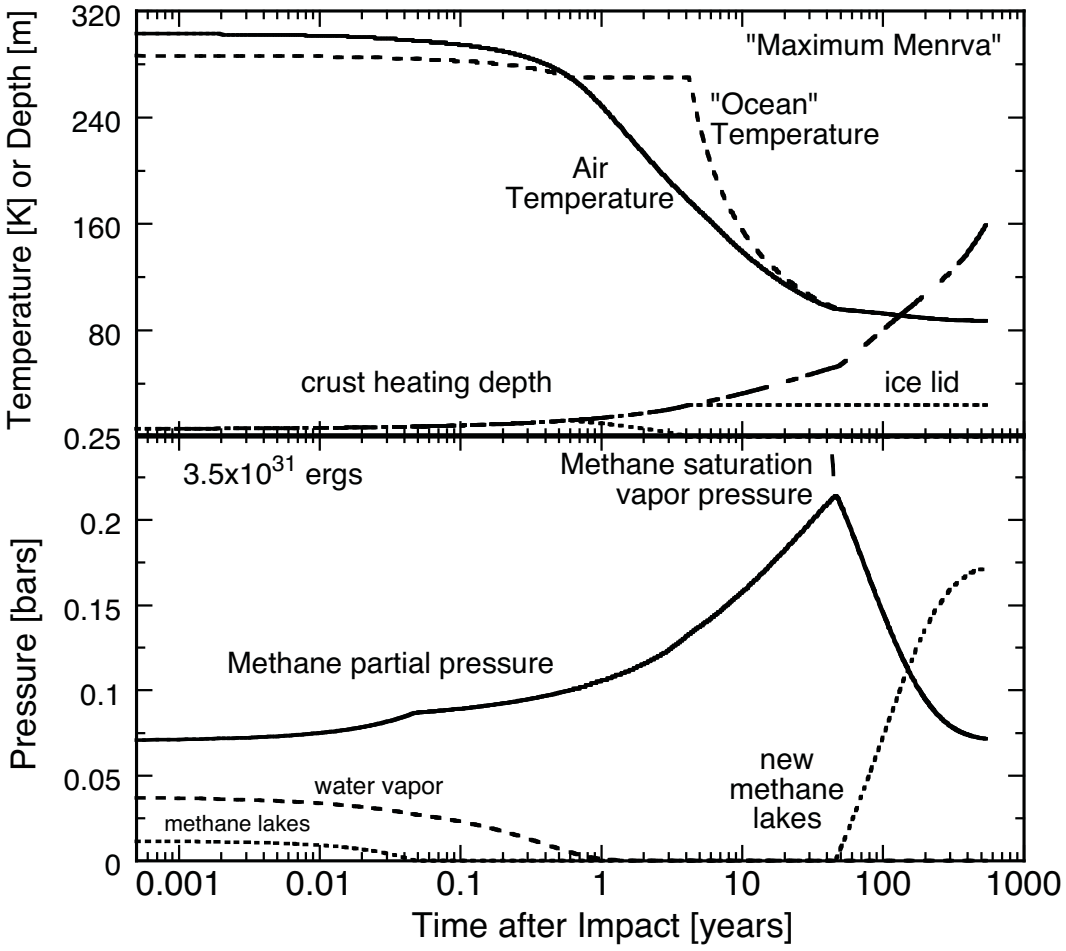
320
240
160
80
0.25
Temperature [K] or Depth [m]
"Maximum Menrva"
"Ocean"
Temperature
Air
Temperature
crust heating depth
ice lid
3.5x10^31 ergs
Methane saturation
vapor pressure
0.2
0.15
0.1
0.05
0
Pressure [bars]
Methane partial pressure
water vapor
methane lakes
new
methane
lakes
0.001
0.01
0.1
1
10
100
1000
Time after Impact [years]

Figure 8:

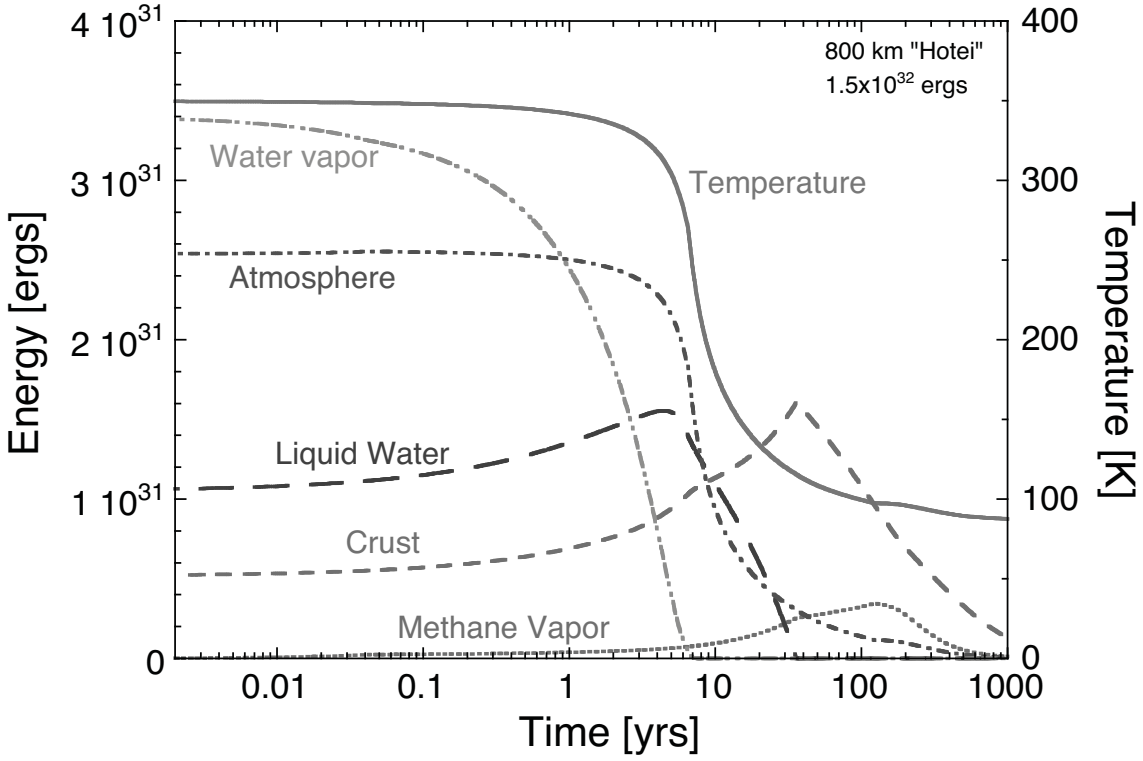
800 km "Hotei"
1.5x10^32 ergs
Water vapor
Temperature
Atmosphere
Liquid Water
Crust
Methane Vapor
Energy [ergs]
Temperature [K]
Time [yrs]
4 10^31
3 10^31
2 10^31
1 10^31
0
400
300
200
100
0
0.01
0.1
1
10
100
1000

Figure 9:

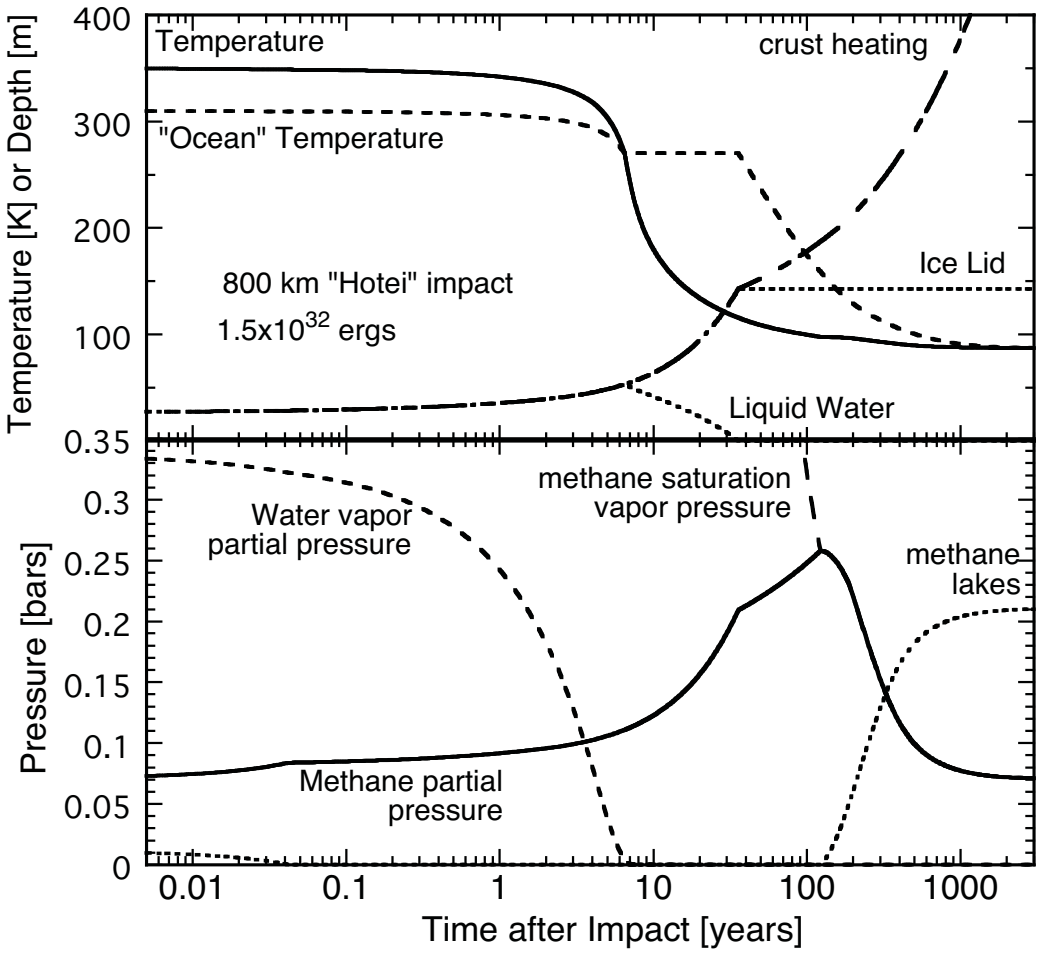
Temperature
crust heating
"Ocean" Temperature
Ice Lid
800 km "Hotei" impact
1.5x10^32 ergs
Liquid Water
Temperature [K] or Depth [m]
400
300
200
100
0.35
methane saturation
vapor pressure
Water vapor
partial pressure
methane
lakes
Methane partial
pressure
Pressure [bars]
0.3
0.25
0.2
0.15
0.1
0.05
0
0.01
0.1
1
10
100
1000
Time after Impact [years]

Figure 10:

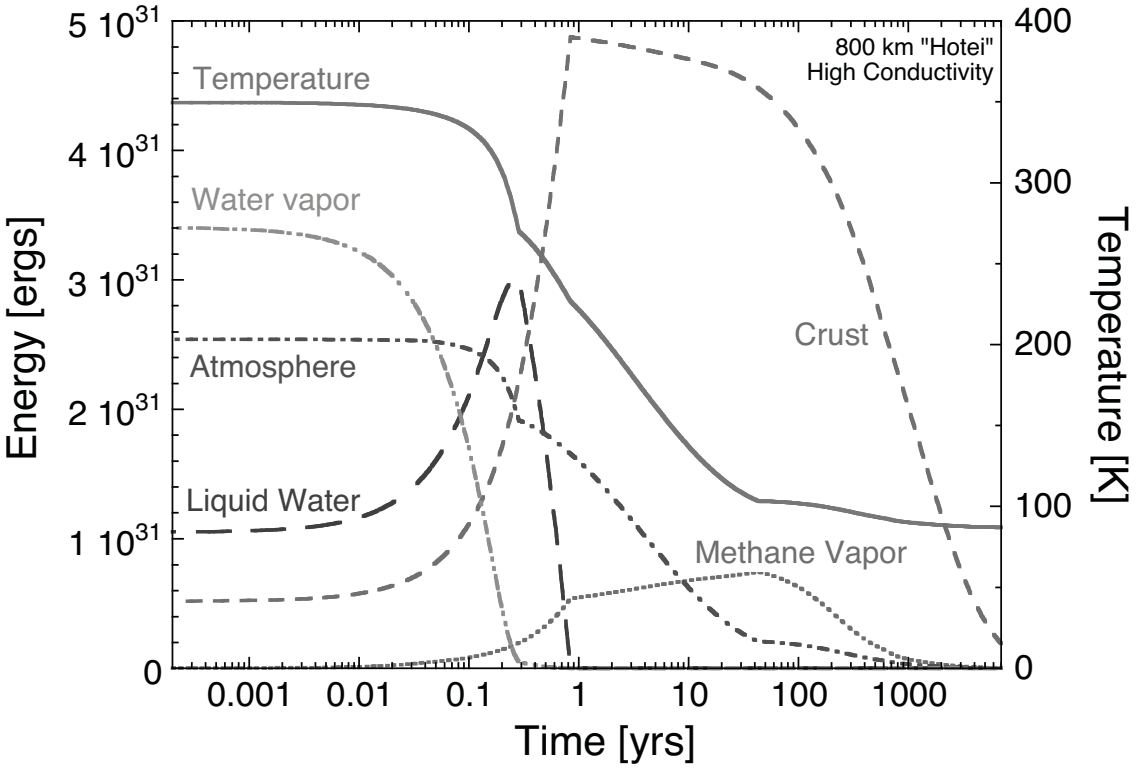
800 km "Hotei"
High Conductivity
Temperature
Water vapor
Atmosphere
Liquid Water
Crust
Methane Vapor
Energy [ergs]
Temperature [K]
Time [yrs]
5 10^31
4 10^31
3 10^31
2 10^31
1 10^31
0
400
300
200
100
0
0.001
0.01
0.1
1
10
100
1000

Figure 11:

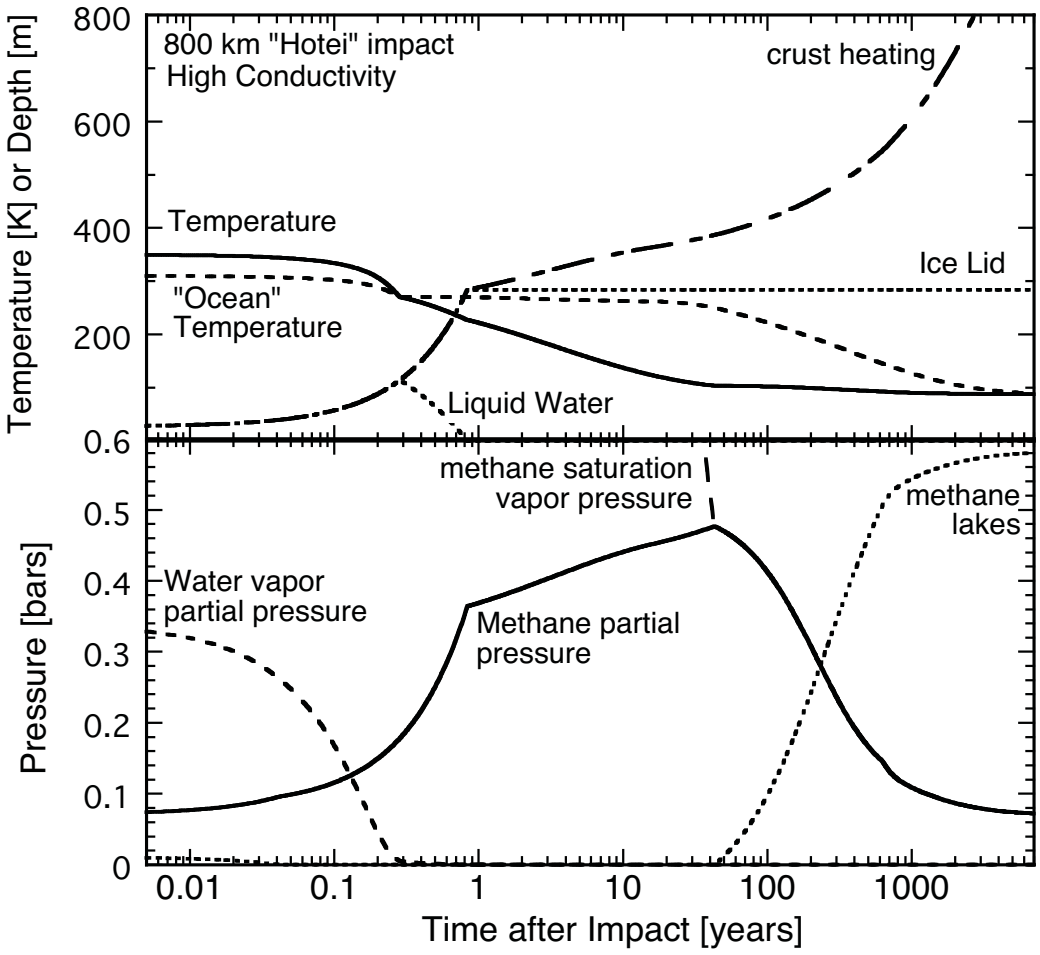
800 km "Hotei" impact
High Conductivity
crust heating
Temperature
Ice Lid
"Ocean"
Temperature
Liquid Water
Temperature [K] or Depth [m]
800
600
400
200
0.6
methane saturation
vapor pressure
methane
lakes
Water vapor
partial pressure
Methane partial
pressure
Pressure [bars]
0.5
0.4
0.3
0.2
0.1
0
0.01
0.1
1
10
100
1000
Time after Impact [years]

Figure 12:

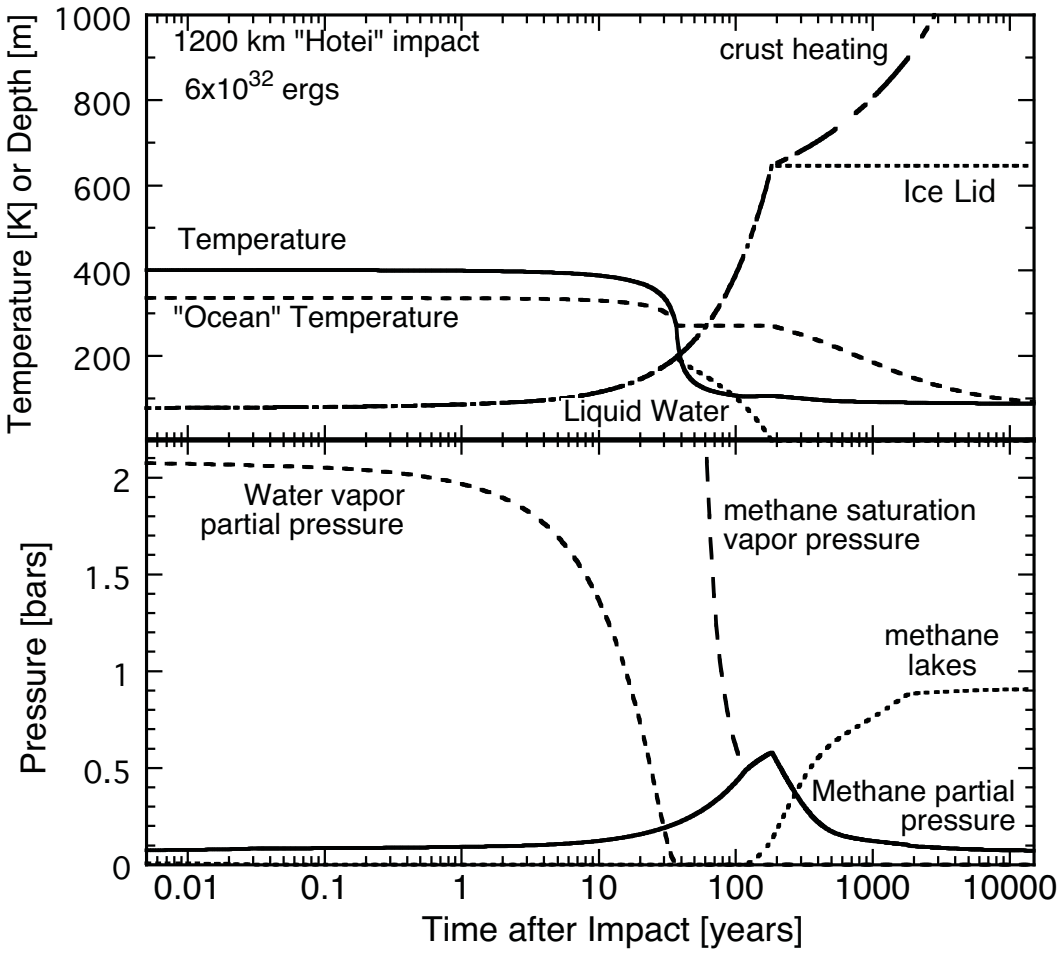
1200 km "Hotei" impact
6x10^32 ergs
crust heating
Ice Lid
Temperature
"Ocean" Temperature
Liquid Water
Temperature [K] or Depth [m]
1000
800
600
400
200
Water vapor
partial pressure
methane saturation
vapor pressure
methane
lakes
Methane partial
pressure
Pressure [bars]
2
1.5
1
0.5
0
0.01
0.1
1
10
100
1000
10000
Time after Impact [years]

Figure 13:

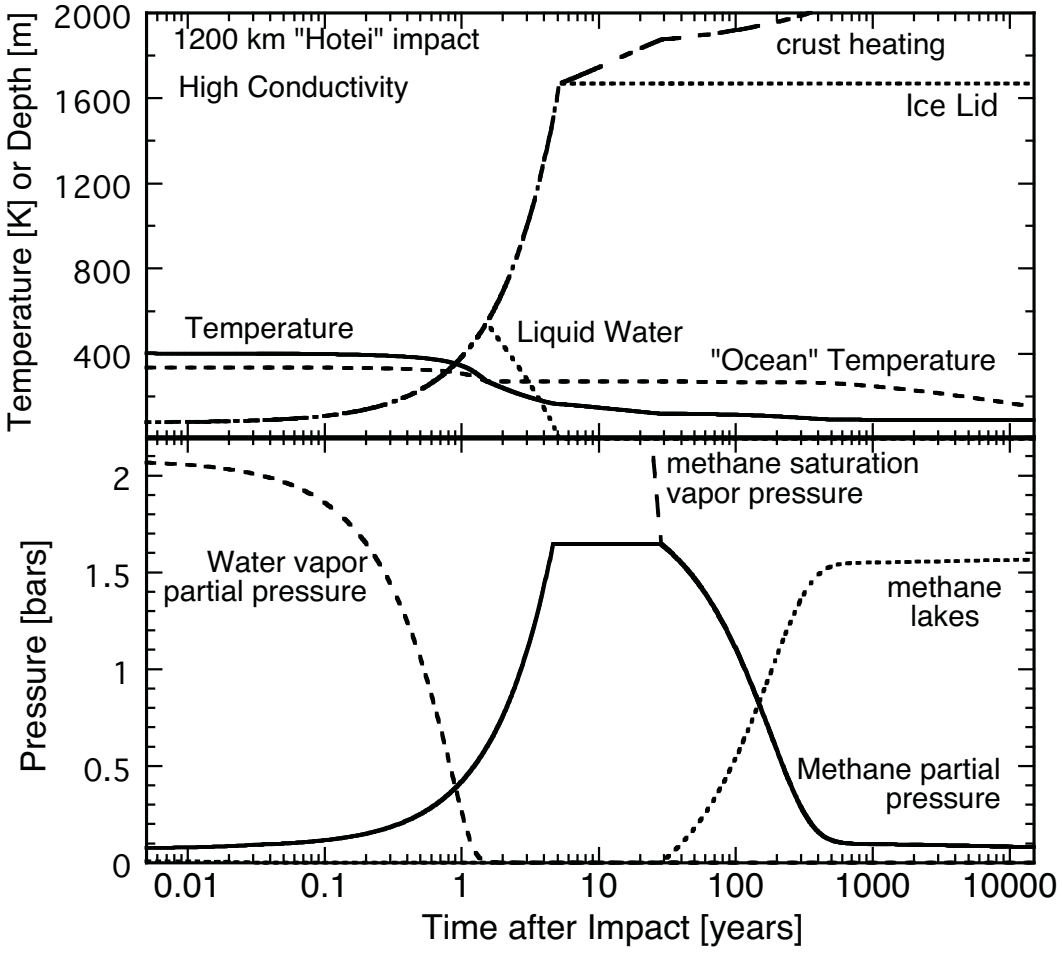
1200 km "Hotei" impact
High Conductivity
crust heating
Ice Lid
Temperature
Liquid Water
"Ocean" Temperature
Temperature [K] or Depth [m]
2000
1600
1200
800
400
methane saturation
vapor pressure
Water vapor
partial pressure
methane
lakes
Methane partial
pressure
Pressure [bars]
2
1.5
1
0.5
0
0.01
0.1
1
10
100
1000
10000
Time after Impact [years]

Figure 14:

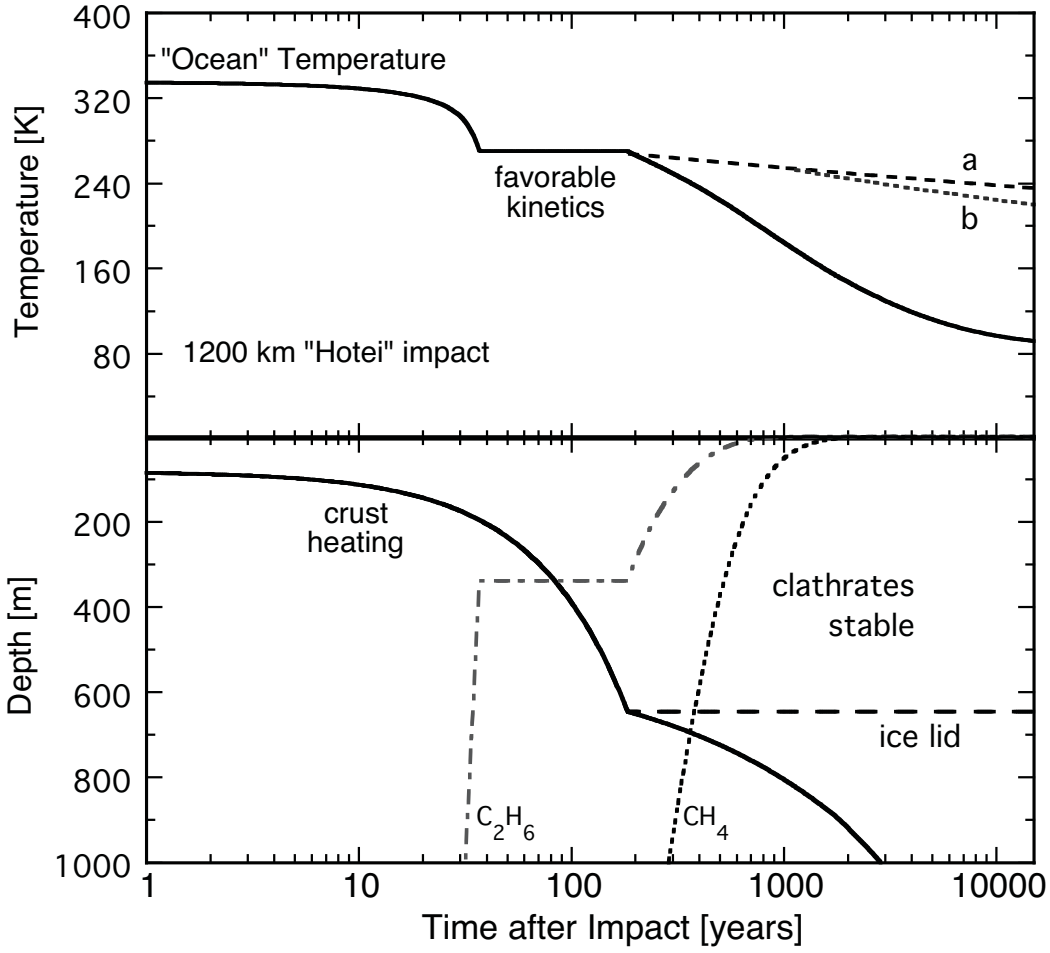
"Ocean" Temperature
favorable
kinetics
a
b
1200 km "Hotei" impact
Temperature [K]
400
320
240
160
80
crust
heating
clathrates
stable
ice lid
C_2H_6
CH_4
Depth [m]
200
400
600
800
1000
1
10
100
1000
10000
Time after Impact [years]

Figure 15:

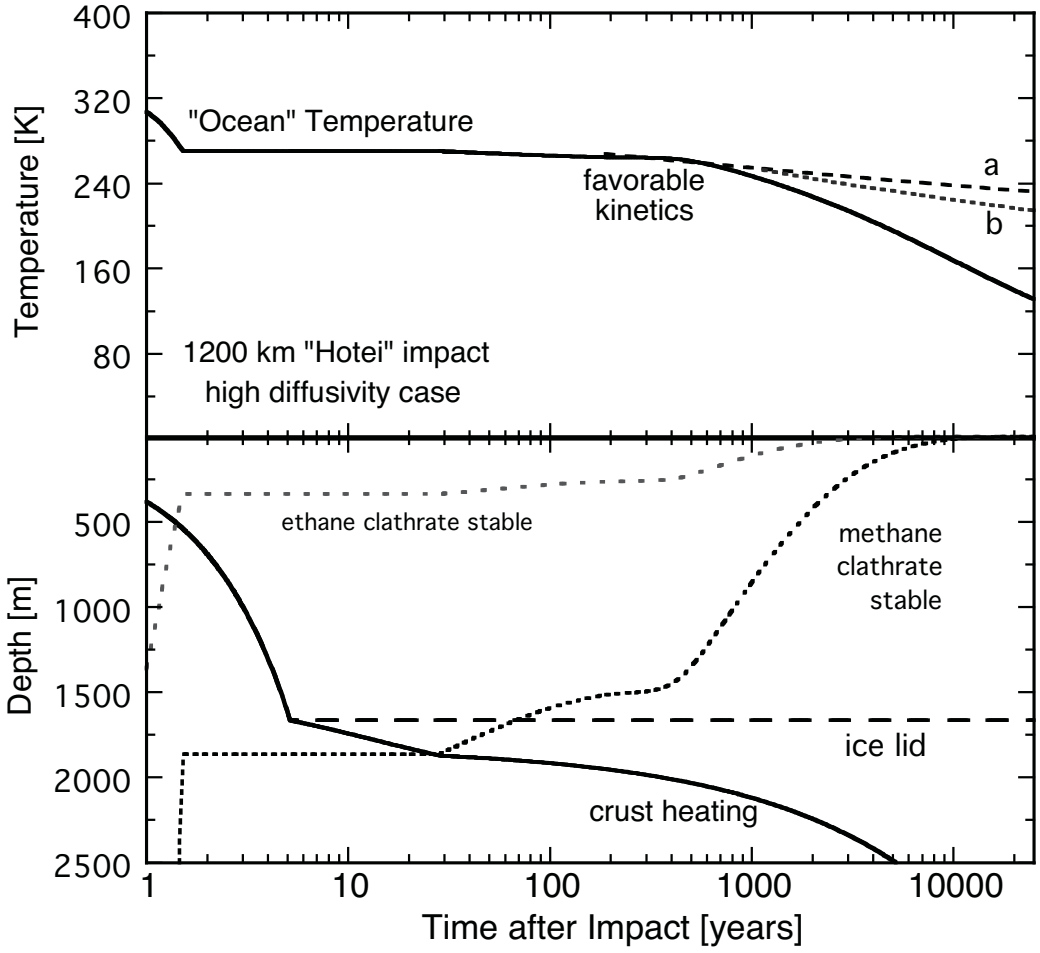
400
320
240
160
80
Temperature [K]
"Ocean" Temperature
favorable
kinetics
a
b
1200 km "Hotei" impact
high diffusivity case
ethane clathrate stable
methane
clathrate
stable
ice lid
crust heating
500
1000
1500
2000
2500
Depth [m]
1
10
100
1000
10000
Time after Impact [years]

Figure 16: